Journal of Hydrology (2007) 337, 294–314

available at www.sciencedirect.com

ScienceDirect

journal homepage: www.elsevier.com/locate/jhydrol

The hydrochemical evolution of brackish groundwater in central and northern Sinai (Egypt) and in the western Negev (Israel)

E. Rosenthal [a,b,*], M. Zilberbrand [b], Y. Livshitz [b]

[a] *Department of Geophysics and Planetary Sciences, Tel Aviv University, Ramat Aviv, Tel Aviv 69978, Israel*
[b] *Hydrological Service of Israel, P.O. Box 36118, Jerusalem 91360, Israel*

Received 27 July 2006; received in revised form 30 January 2007; accepted 31 January 2007

KEYWORDS
Trans-boundary groundwater resource
Sinai (Egypt);
Negev (Israel);
Paleowater;
Hydrochemical modeling;
Neogene erosional channels

Summary Cretaceous trans-boundary aquifers in the central and northern parts of Sinai (Egypt) and the Negev (Israel), are geographically and geologically both contiguous and continuous. Hydrogeological and hydrochemical studies of these aquifers, with disregard to political boundaries, are scarce. The Lower Cretaceous Kurnub Group aquifer in Sinai and the Negev hosts paleowater mostly replenished during the Pleistocene. The objectives of this study are to elucidate the relationship between regional structural elements and the salinization of groundwater in the Kurnub Group in Sinai and further downstream in the Negev.

The stable plateaus in southern Sinai and the fold structures in the north continuing into the Negev are separated by the W–E striking Minshara–Ramon shear zone. With the exception of higher salinities in the north, the chemical composition of Kurnub Group groundwater north and south of the shear zone is similar. Similarly, groundwater in the overlying Upper Cretaceous aquifer differs from Kurnub groundwater only within and north of the shear zone and is characterized by higher Cl concentrations, lower Mg/rCa ratios (due to high Ca in the calcareous aquifer) and by a ''heavier'' isotopic signature. Inverse hydrogeochemical modeling using PHREEQC indicates that the increase in salinity of Kurnub groundwater within the shear zone and in adjacent areas could be due to two different sources: First, the salinization process could be the result of mixing with sulfate-rich brackish groundwater occurring in Jurassic formations, which are in fault-controlled lateral contact with the Kurnub Group aquifer. Second, the salinity differences could be from unflushed seawater in the subsurface of the northern Sinai and western Negev, i.e. possible remnants of the post-Messinian (Lower Pliocene) transgression, which penetrated into northern Sinai, the western Negev and the Coastal Plain of Israel both through ero-

* Corresponding author. Address: Hydrological Service of Israel, P.O. Box 36118, Jerusalem 91360, Israel.
E-mail addresses: elirose@netvision.net.il (E. Rosenthal), michaelz20@water.gov.il (M. Zilberbrand), yakovl20@water.gov.il (Y. Livshitz).

doi:10.1016/j.jhydrol.2007.01.042

sional channels, which were incised during the Neogene, and by flooding over outcrops of permeable formations.

Background

The central and northern parts of Sinai (Egypt) and the Negev (Israel) are geographically and geologically both contiguous and continuous (Fig. 1). The Lower Cretaceous Kurnub Group aquifer occurs in the subsurface of these two geographical areas and contains paleowater, which was mostly replenished during the Pleistocene (Issar et al., 1972; Issar, 1981). These authors and others (Said, 1962, 1990; Kroitoru, 1980; Weinberger et al., 1992; Rosenthal et al., 1998) outlined the inferred flow paths connecting the natural replenishment areas in the Sinai highlands with the natural outlets in Israel, and modeled the processes which shape the chemical composition of this paleowater. The amount of available data is rather limited. However, by considering hydrogeological and hydrochemical evidence published during the last decade (Abd Allatif and Galal, 1997; Abd el Samie and Sadek, 2001; Fekry, 2001; Zaghloul, 1999) and by

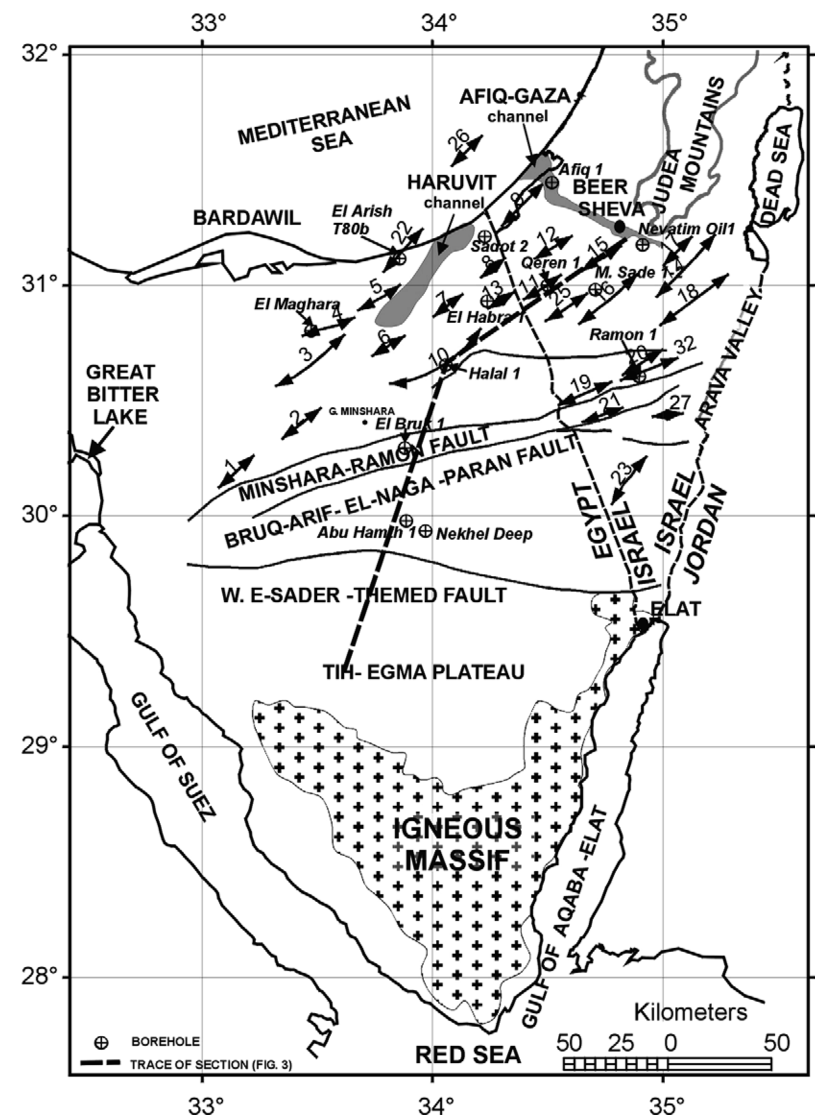

Figure 1 Structural location map indicating the main anticlines in Sinai and in the Negev, the main faults and the subsurface traces of the erosive channels (modified and schematized after Eyal et al., 1987 and Jenkins, 1990). 1 — Giddi; 2 — Yelleg; 3 — El Maghara; 4 — Um Mofruth; 5 — Risan Aneiza; 6 — Libni; 7 — Succot; 8 — Sadot; 9 — Nirim; 10 — Halal; 11 — Qeren; 12 — Haluza; 13 — Habra; 14 — Hatira; 15 — Hazerim; 16 — Boqer; 17 — Dimona; 18 — Hazera; 19 — Ramon; 20 — Mahmal; 21 — Arif; 22 — El Arish; 23 — Zenifim; 25 — Shivta; 26 — Till; 27 — Eshet; 32 — Inmar.

ascertaining the regional distribution of data, it is possible to outline an updated regional model of salinization of the paleowater which flow from NE Sinai to the Negev forming a major, regional trans-boundary groundwater resource.

The chemical evolution of the Kurnub Group paleowater was investigated by Rosenthal et al. (1998) starting from rainwater in recharge areas in Sinai and along groundwater flow paths leading to the natural outlets of this regional aquifer. This was achieved by modeling of both rock/water interaction and mixing with brines mainly close to the natural outlets in the Dead Sea area and along the Arava Valley. The previous hydrochemical modeling (Rosenthal et al., 1998) showed that the Kurnub Group paleowater in the central parts of the Negev could be derived from the paleowater in Sinai mainly by dissolution of halite, plagioclase, organic matter and goethite and by precipitation of calcite, Ca-smectite, silica and pyrite. The chemical composition of Kurnub Group groundwater encountered in wells located close to the Dead Sea evolved as the result of mixing of the Kurnub groundwater of the central Negev with typical Ca-chloride water of the Rift.

Objectives

Whereas earlier there was no available data which could have related the previously mentioned hydrochemical processes to regional geological and structural features, by examining the chemical evolution of Kurnub-Group paleowater in the Sinai—Negev area against the geostructural background, we are now able to present information here which complements previously published results (Rosenthal et al., 1998).

The objectives of this study are to elucidate the relationship between regional structural elements and the salinization of groundwater in the Kurnub Group in Sinai and further downstream in the Negev.

Climatic conditions

Central and northern Sinai and the southern Negev are arid areas with scarce and irregular seasonal rainfall. In Sinai the precipitation ranges between 40 mm/yr at Nekhel Deep (Fig. 1) and 200 mm/yr near the Mediterranean coast (Abd el Rahman, 2001; El Ghazawi, 1992; Zaghloul, 1999; Abd el Samie and Sadek, 2001). Rainfall in the Negev is in the 100—200 mm/yr range. Potential evaporation exceeds 2400 mm/yr in Sinai and 1400—1800 in various parts of the southern Negev (Abd el Samie and Sadek, 2001; Gvirtzman, 2002). Due to these extreme climatic conditions, current replenishment of groundwater (if at all) is very limited (Abd el Rahman, 2001). Limited replenishment of groundwater could be due to infiltration of winter flash floods into the dry stream-beds of the area (Abd el Rahman, 2001).

The geological environment — literature review

The study area is located on the northward dipping margins of the Arabo-Nubian massif which is covered by a sedimentary veneer (Kashai et al., 1987). Three main morpho-tectonic units are discerned (Jenkins, 1990; Abd el Samie and Sadek, 2001):

- the southern igneous and metamorphic core;
- the plateaus of Gebel E-Tih and El Egma built of sub-horizontal, Lower Cretaceous Nubian sandstones overlain by Middle-Cretaceous to Paleocene calcareous formations,
- the northern alluvial plains broken by parallel domes and by anticlines which continue into the Negev, trend north-eastwards and make a part of the huge Syrian Arc system (Jenkins, 1990).

The transition zone between the stable plateaus in the south and the fold structures in the north is outlined by four major displacements extending E—W and NE—SW and continuing from Sinai into the Negev (Eyal et al., 1987). The southern displacement is the E—W trending Themed—Wadi E-Sader fault (also known as the Themed—Ragabet el Naam fault). Further northward, the shear-zone is built of three parallel NE—SW trending fault zones (Fig. 1), i.e. the Buruq—Arif el Naga—Paran fault, which reaches in the east to the Arava Valley and Dead Sea Rift (Eyal et al., 1987; Kashai et al., 1987). Further northward is the Minshara—Ramon fault which like the others is a dextral strike-slip fault with horizontal displacement of 0.4—2.2 km. Vertical displacements may reach 1000 m, particularly in the central part of the shear zone (Bartov, 1974; Eyal et al., 1987; Jenkins, 1990). Considerable thickening of the whole Triassic-Tertiary sedimentary sequence occurs north of the transition zone. Numerous faults dissect this transition zone creating horst-and-graben and dome-like structures. According to Kashai et al. (1987) the folded zone extending north of the shear zone includes four parallel sequences of anticlinal structures, generally striking NE—SW (Fig. 1).

The continental shelf and the subsurface of the coastal plain of Sinai and of Israel are deeply incised by 10 erosive channels, which were part of the Neogene drainage system (Gvirtzman and Buchbinder, 1977; Fleischer et al., 1993). These channels truncate large portions of the Cretaceous section reaching, in many cases, close to the base of the lower Cretaceous Kurnub Group. The channels are filled by very thick sections (>1000 m) of clastics and evaporites such as anhydrite and halite of the Messinian age (the Tertiary Saqiye Group), and are overlain by argillaceous beds related to the upper part of the Saqiye Group (Gvirtzman and Buchbinder, 1977; Fleischer et al., 1993). Two such erosive channels occur in the study area. In Sinai, the *Haruvit channel* extends in the subsurface from the shelf, 50 km southwestwards inland extending between the anticlines of Sadot, Succot and Risan Aneiza. The channel is filled by a 1100 m thick sequence of clastics and evaporites, especially anhydrite. In the deepest parts of the channel there are minor occurrences of halite (Fleischer, 1979). In Israel, the *Afiq-Gaza channel* extends also from the shelf eastwards towards Beer Sheva and truncates Paleogene to the lower part of the Lower Cretaceous rock formations. The lithology of the fill material in the Afiq-Gaza channel resembles that of the Haruvit channel.

The regional stratigraphic sequence relevant to the present discussion is shown in Fig. 2. The following units are of particular hydrogeological interest.

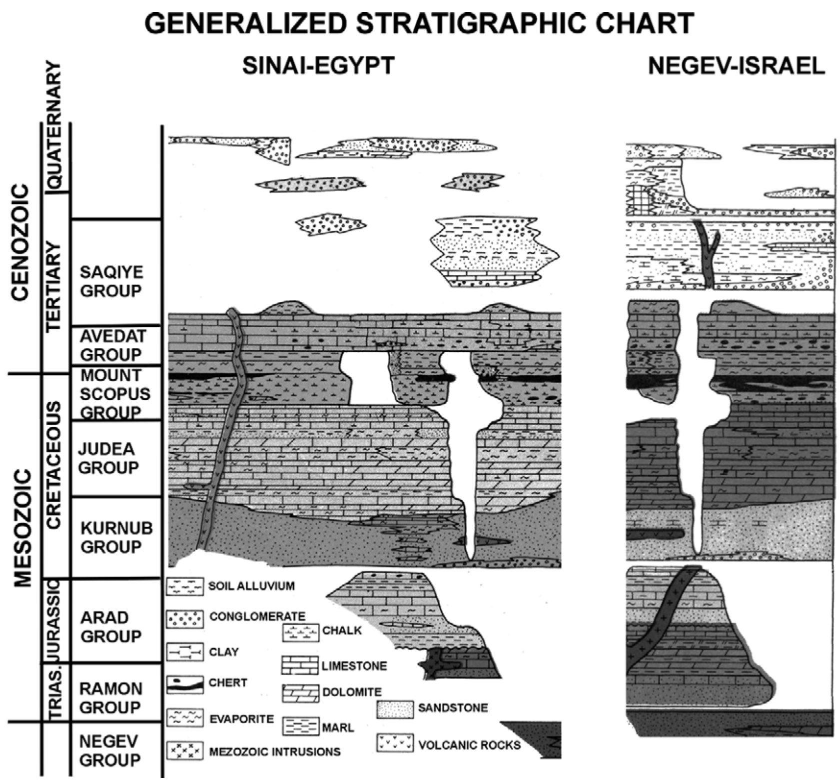

Figure 2 Generalized stratigraphic chart for Sinai and the Negev (modified after Bartov et al., 1981; Eyal et al., 1980).

In the Negev, in borehole Ramon 1 and in exposed sections, the 207 m thick *Upper Triassic Mohilla* beds contain massive layers of gypsum. The massive development of gypsum, which is characteristic for the Negev, does not occur in Sinai (Druckman, 1987; Kashai et al., 1987).

In the El Maghara Mountains and in borehole Halal 1 *the Jurassic sequence* was investigated by Said (1962, 1990), Goldberg et al. (1971), Goldberg and Raab (1987) and Lapidoth (1976). The thick sections (2050 m in El Maghara and up to 3100 in the borehole) contain a variety of lithologies such as limestones and dolomite, sandstones, shales and chert and abundant veins of secondary anhydrite, barite and/or celestite. In the Negev the thickness of Jurassic formations in boreholes (of similar lithologies) varies between 1155 and 2273 m. Mills and Shata (1989) defined the aquiferous beds in the Jurassic sequence in Sinai as ''good to fair'' water sources with a mean TDS-content of 6000 mg/l. Due to the occurrence of major faults (the Minshara shear-zone and faults north of the Halal Mts.), brackish water originating from Jurassic beds may flow laterally into the permeable sandstones of the Lower Cretaceous Kurnub Group (Mills and Shata, 1989). Nada and Awad (1991) also suggested that due to the absence of impervious beds between the Jurassic and Lower Cretaceous in Sinai, interaquifer flow could occur between these rock-units.

The Lower Cretaceous Kurnub Group, which is a part of the Nubian Sandstone sequence, comprises mainly sands and sandstones often interbedded with marine sediments. Farther from the Arabo-Nubian massif, north of the El Maghara — Halal Mts. and into the western Negev, lithology changes from prevalently terrestrial to carbonates and shales of increasingly marine facies (Rosenthal et al., 1992; Water Resources Research Institute and Japan International Cooperation Agency, 1992; Abd el Rahman, 2001). In Sinai, the southern boundary of the aquifer outcrops is on the E-Tih and El Egma plateaus (Issar et al., 1972; Abd el Samie and Sadek, 2001). The aquifer extends also eastwards to the Dead Sea and the Rift Valley (Issar et al., 1972; Rosenthal et al., 1998) and north-eastwards into the Negev (Weinberger et al., 1992). The total thicknesses of the Kurnub Group in Sinai varies between 180 m in the south and in the Arif el Naga area (The Malha Fm. — Zaghloul, 1999) and 250 m in the central part (Nekhel Deep, Themed and Kuntila) and reaching a maximum of 520 m at Halal (Abd el Samie and Sadek, 2001). In Israel the thickness of the terrestrial beds of the Kurnub Group is close to 250—300 m (Weinberger et al., 1992).

The Upper Cretaceous sequence is known in Israel as the *Judea Group*. It is prevalently built of limestone and dolomite beds unconformably deposited over the underlying Kurnub Group. The thickness of these beds close to the northwestern scarp of the E-Tih plateau is 190 m increasing gradually north and northeastward. In the northernmost on- and offshore boreholes of Sinai, Judea Group beds are absent as a result of erosion (Kashai et al., 1987; Jenkins, 1990). In the western Negev the total thickness of these beds varies between 600 and 700 m (Fleischer et al., 1993) whereas in the Judea Mountains of Israel, hundreds of meters of permeable Aptian—Albian limestones separate the Judea and Kurnub Groups. Due to this lithostratigraphic feature, the Judea and the Kurnub Groups form one hydrological unit (Arad, 1964; Arad and Kafri, 1980). In the northern Negev and in northeastern Sinai, the Judea Group aquifer either directly overlies the Kurnub Group or is separated from it by a thin sequence of marls and limestones where only a small vertical displacement is required to bring the two aquifers in contact. In Sinai no impervious beds separate the two aquifers and therefore hydraulic interconnection and inter-aquifer flow are possible. This is also facilitated by the numerous faults dissecting the area.

The hydrogeological environment

According to Issar et al. (1972) and Issar (1981) the Kurnub Group aquifer in Sinai and in the Negev contains paleowater which accumulated mostly during the Pleistocene. The recharge of meteoric water may have taken place mainly over sandstone outcrops on the E-Tih and El Egma plateaus in Sinai. During the Pluvial, replenishment to the Kurnub-Group aquifer could have taken also place over the major breached anticlines in which the exposed cores consist of sandy beds of the Kurnub Group. Such processes occur in the Halal, Arif el Naga, El Maghara, Minshara, and Yelleg mountains, over the shallow-buried El Arish fold structure in Sinai, and over the Ramon, Hatira and Hazera structures in the Negev. Throughout most of Sinai, there are no impervious beds separating the Upper Cretaceous (Cenomanian and Turonian) beds and the underlying sandy Kurnub Group sequence. Precipitation in the past and at present could have reached the Kurnub aquifer by direct infiltration through the overlying calcareous beds. According to Arad and Kafri (1980), in those areas in which there is no lithological separation between the two aquifers, the exposures of the Judea Group must be also regarded as natural replenishment areas for the Kurnub Group aquifer. At present, the Cretaceous Halal and Wata limestone formations in Sinai and the aquiferous units of the Judea Group in the Negev are occasionally and locally recharged from storm run-off (Arad and Kafri, 1980; Zaghloul, 1999).

Abd el Rahman (2001) estimated the average storage capacity of the Kurnub Groups aquifer at 299×10^9 m^3. Abd el Samie and Sadek (2001) estimated the current recharge in Sinai at 4.8×10^6 m^3/yr. The current recharge over outcrops in the Negev is of similar order (Kroitoru, 1980).

The Kurnub Group is not the only aquifer in the study area. Groundwater — mostly brackish — occurs in the Upper Cretaceous (Judea Group) beds of central and northern Sinai and in the western Negev. Rosenthal et al. (1998) showed that in the western Negev, these brackish waters are mixing products of Kurnub-Group water with fresh water replenished on the southern plunges of the Judea Mountains and flowing southward to the western Negev.

Flow paths in the Kurnub and Judea Group aquifers

According to Issar et al. (1972) and to Rosenthal et al. (1998), groundwater in the Kurnub Group aquifer in Sinai and in the Negev spreads fan-wise towards the natural outlets of the aquifer i.e. the Gulf of Suez, the northwestern Negev, the Dead Sea, and the Gulf of Aqaba-Elat.

At this stage there is no sufficient information neither on the regional continuity of the Upper Cretaceous Judea Group groundwater body in Sinai, nor on its flow directions and its natural outlets. Baida et al. (1978) assumed that the Judea Group in northern Sinai forms a part of the large Yarkon-Taninm groundwater basin extending to the western Judean Mountains. Bar Joseph (1978) suggested an outlet (for groundwater flowing in the Judea Group from Sinai towards Beer Sheba) through the Afiq-Gaza channel to the Mediterranean Sea.

Lateral inter-connections between aquifers in fault zones

As mentioned previously, the irregular pattern of displacement along the Themed—Wadi e-Sader fault, funnels the flow of paleowater from their recharge areas on the plateaus, towards Nekhel Deep and further northwards. The transition zone extending between the Themed—Wadi e-Sader fault in the south and the Buruq—Arif el Naga—Paran fault, is also dissected by numerous faults disturbing the continuity of the Kurnub Group aquifer. This is clearly illustrated by geological sections by Kashai et al. (1987), Jenkins (1990) and Abd el Samie and Sadek (2001). The typical cross-section along the

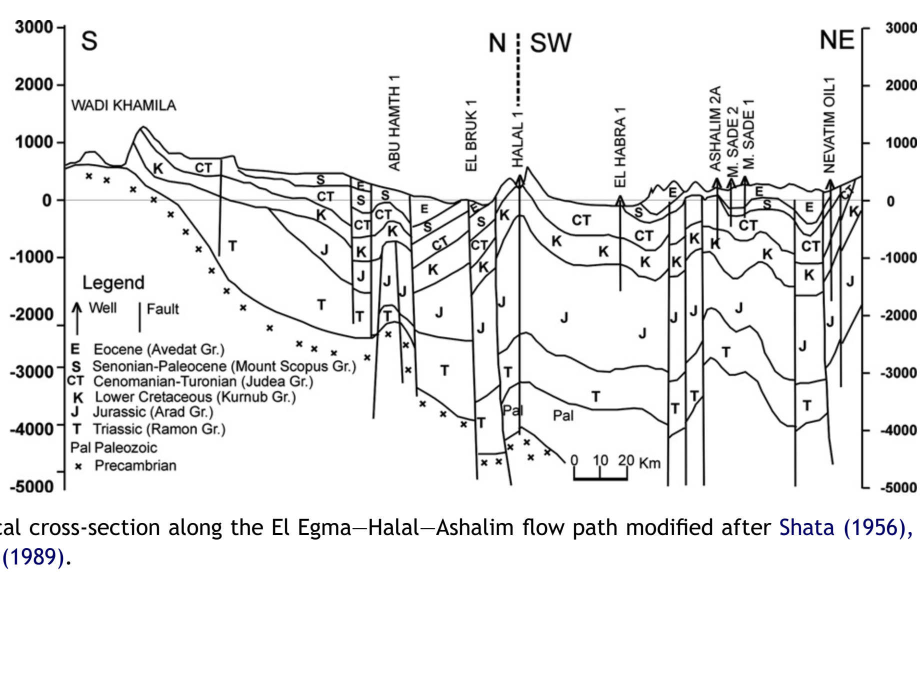

Figure 3 Geological cross-section along the El Egma—Halal—Ashalim flow path modified after Shata (1956), Kashai et al. (1987) and Mills and Shata (1989).

main flow path from central Sinai into the Negev is presented in Fig. 3. Accordingly, in central Sinai, in the transition zone between Abu Hamth 1 and El Bruk 1, a major fault positions Upper Cretaceous calcareous beds of the downthrown block against the sandstones of the Kurnub Group, thus facilitating lateral inflow of paleowaters into the calcareous aquifer. Similar situation occurs further northwards, between Arif el Naga and Halal. North of El Bruk 1, major displacements create similar geological conditions facilitating possible inter-aquifer flow between Jurassic, Lower Cretaceous and younger rock units. By considering mostly isotope data, Hening et al. (2005) suggested that in northeastern Negev, a large volume of Jurassic sulfate-rich groundwater contribute locally to the Kurnub Group aquifer.

The flow pattern

Considering the contribution of numerous authors (Issar et al., 1972; Kroitoru, 1980; Kronfeld et al., 1993; Rosenthal et al., 1998; Abd el Samie and Sadek, 2001) and in view of structural evidence by Bartov (1974), Eyal et al. (1987), Kashai et al. (1987) and Jenkins (1990), the pattern of paleo-groundwater flow in Sinai and in the Negev is controlled by structural and lithostratigraphic factors as summarized below.

According to Abd el Samie and Sadek (2001), in the area between the El Tih and El Egma plateaus and the shear zone, groundwater flows in the Kurnub Group aquifer from the eastern parts of the El Egma plateau north-westwards and northwards. The flow is from +467 m above MSL (Wadi Sheira well) to +200 m in the Jica 1 and Nekhel Deep wells and further to El Halal +24 m (Fig. 4). Relatively high water levels (up to +250) have been observed in the Bir El Themade and El Bruk 1 wells located at the western extremity of the shear zone. Groundwater flow northward towards Nekhel occurs mainly across those portions of the Themed—Wadi e-Sader fault where fault displacement is minimal. The flow of paleowater is then diverted towards the Negev and to the Rift Valley and westwards to the Gulf of Suez and the Great Bitter Lakes (Issar et al., 1972). Together with paleowater recharged on the Halal structure, the flow continues within the Kurnub Group aquifer through the synclinal troughs, north-eastwards into the western Negev and towards the Dead Sea.

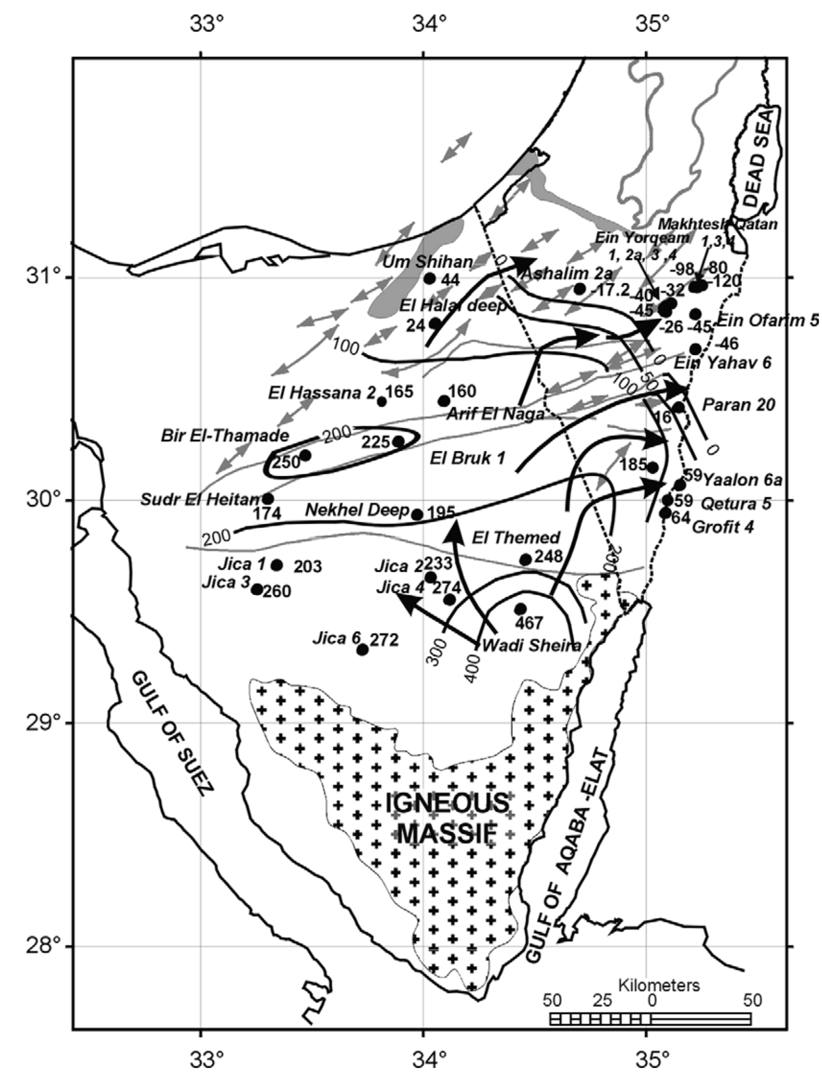

Figure 4 Groundwater elevation (related to MSL) and inferred flow paths in the Kurnub Group aquifer from Sinai to the Negev.

The geological, structural and hydrological data accumulated during the last decade on both sides of the international border, enables now to propose an updated and more detailed model of paleowater flow from Sinai to the Negev and further to the eastern drainage bases. It appears that the dominant factors of this model are the Minshara – shear zone and the uplifted Ramon anticlinal structure. In the Negev, the Ramon structure creates a major structural watershed, which divides the great mass of paleowater into two water bodies. One body of paleowater flows from Sinai across the eastern part of the Themed–Wadi e-Sader fault and then, by following the synclinal troughs between the Ramon, Eshet and Zenifim anticlines in southeastern Negev, the water flow to the southern Arava Valley and finally to the Red Sea (Fig. 4). Groundwater elevations are +467 m in Sinai Wadi Sheira, +248 m at El Themed, +185 m at Shizafon in the eastern Negev and as low as +50 m in well Qetura 5 in the Arava Valley (Fig. 4). The other mass of paleowater seems to pass from Sinai to the Negev by flowing across the Minshara shear-zone possibly in the area between the western plunge of the Ramon structure. The flow to the northern Arava Valley and to the Dead Sea is in the synclinal troughs: between and in parallel to the axes of the major anticlinal structures of the Negev, such as Mahmal, Hazera, Hatira and other structures, as shown in Fig. 1. Along the flow path to the Dead Sea, water levels decline from −28.5 m to as low as −285 m (along the western shore of the Dead Sea). North of the Minshara–Ramon structural watershed, paleowater probably replenished over the Halal structure, flows northeastwards, towards central Negev, attaining there a piezometric level of −14.7 m (well Ashalim 2a).

Due to facies changes and major reverse folding, which create impermeable barriers, paleowaters do not flow in the subsurface to the Mediterranean Sea (Weinberger et al., 1992). Because of lithological considerations, Issar et al. (1972) excluded flow of paleowater from Sinai to the western Negev. However, following the formulation of an updated subsurface geological model and after reassessing its hydrogeological aspects, Weinberger et al. (1992) and Rosenthal et al. (1998) concluded that in the western Negev, the Kurnub Group should also be regarded as an aquifer and as a potential source of groundwater. Moreover, specific local lithologic and structural conditions facilitate lateral flow of Kurnub paleowater into the Judea Group.

There are no sufficient data to draw a reliable map of groundwater levels in the Upper Cretaceous beds of Sinai. Over vast parts in the western Negev, piezometric levels in autumn 2004 were in the +15 to +17.5 m range.

The chemical composition of groundwater

The chemical composition of groundwater in the study area is given in Table 1.

Ionic ratios were used as a useful tool for comparing different water bodies and for tracing the geochemical evolution of groundwater. This technique was suggested by Schoeller (1956) and White (1960). The significance of the computed ratios is described in detail by Rosenthal (1987).

Groundwater in the Kurnub Group aquifer is characterized by high sulfate concentrations. The average rSO_4/rCl ratio is 0.65, with maximal values reaching 1.09–2.11. Only in well El Bruk 1, the rSO_4/rCl ratio drops below the marine value of about 0.1. By applying the Pearson's correlation matrix for major ions, pH and $\delta^{18}O$ (Table 2) it occurs that strong correlation ($R = 0.875$) exists between sulfate and both calcium and magnesium concentrations. Comparing equivalent calcium and sulfate concentrations reveals that they are close to the ''$CaSO_4$ line'' ($rCa^{2+} = rSO_4^{2-}$ – Fig. 5). This fact hints to strong influence of dissolution of calcium sulfate. In those parts of the aquifer, where carbonates prevail, $rCa^{2+} < rSO_4^{2-}$. Such a relationship could be caused by precipitation of carbonate. However, even in this domain, there is a strong correlation between calcium and sulfate concentration.

The chemical changes from rain- to groundwater were modeled by Rosenthal et al. (1998). The model indicates that when rainwater percolates into the subsurface, the chemical composition reflects both dissolution of gypsum, halite, dolomite, Mg-salts and K-feldspar, precipitation of calcite, SiO_2, Ca-smectite, and degassing of CO_2.The origin of the dissolved minerals is from the lithology of the Kurnub Group (Weinberger, 1986). According to Starinsky et al. (1983) $MgCl_2$ is considered to represent marine aerosol occurring over the region.

Table 3 summarizes the average chemical characteristics of Kurnub groundwater south and north of the shear zone. By mapping the groundwater chemistry in the Kurnub Group aquifer (Figs. 6,7 and 8), a very clear zonation stands out. *South of the shear zone*, Cl concentrations are in the range of 122–508 mg/l (average of 290 mg/l). Sulfate concentrations evolve between 60 and 682 mg/l (average of 394 mg/l). Anomalously high sulfate concentrations of up to 560–680 mg/l occur spotwise in different and seemingly unconnected locations, such as in wells Jica 1 and 6 and Sudr El-Heitan (Abd el Samie and Sadek, 2001). The waters are characterized by relatively high pH (up to 8–8.3), and have ionic assemblages of $rNa > rCa > rMg$ and $rSO_4 > rCl > rHCO_3$ or $rCl > rSO_4 > rHCO_3$. The waters are characterized by average rSO_4/rCl and $rSO_4/rHCO_3$ ratios of 1.05 and 2.5, respectively and by $rNa/rCl = 0.91$ and $rMg/rCa = 1.23$. The Cl/Br weight ratio (444) is significantly higher than the marine values (286), and $\delta^{18}O$ and δD are in the −5.9‰ to −8.8‰ and −42.8‰ to −58.6‰ ranges, respectively (see Figs. 8, 9 and 10).

In the shear zone and northward, the Cl concentrations are in the 861–1350 mg/l range, i.e. threefold higher than in the south. In wells Arif el Naga and Um Shihan sulfate concentrations reach 1170 and 2218 mg/l, respectively, whereas pH drops to 7.8, and the water acquire a ionic assemblage of $rNa > rMg > rCa$ and $rCl > rSO_4 > rHCO_3$. The water is characterized by a lower average rNa/rCl ratio (0.72) and a wide range of rMg/rCa ratios of 0.33–1.52. $\delta^{18}O$ is in the −6.04‰ to −9.53‰ range, whereas δD is between −37.3‰ and −52.4‰.

North of the shear zone, the average pH (7.84) is slightly lower than to the south (8.06), whereas the average $\delta^{18}O$ north of the shear zone (−7.28‰) is slightly higher comparing to the southern value (−7.76‰), (Fig. 9). This could be caused by mixing of Kurnub groundwater flowing northeast-

Table 1 Chemical composition and stable isotopes of groundwater

Well_name	Area	Depth, m	Temperature, °C	pH	Ca, mg/l	Mg, mg/l	Na, mg/l	K, mg/l	Cl, mg/l	SO_4, mg/l	HCO_3, mg/l	Br, mg/l	TDS	$\delta^{18}O$	δD	*d*-Excess	RE
Kurnub Group aquifer																	
Jica 3	Sinai, S of the shear zone	980		8.10	60.1	38.9	55	8.7	122	139.9	178.1		603	−8.79	−56.0	14.3	−2.53
Jica 1	Sinai, S of the shear zone	1250		8.20	108.2	92.6	144	16	203	579.7	203.3		1347	−7.87	−58.6	4.4	−3.51
Jica 6	Sinai, S of the shear zone	850		8.10	140.3	121.6	252	12.5	508	559.7	182.9		1777	−5.90	−42.8	4.2	−1.21
Wadi Sheira	Sinai, S of the shear zone	804		8.30	84.2	40.8	147	13.2	326	60	215.5		887	−8.13	−53.2	11.8	1.11
Nekhel deep	Sinai, S of the shear zone	1020		8.00	151	78	218	22	355	530	220	0.80	1575	−7.45	−53.6	6	2.50
Sudr El Heitan	Sinai, S of the shear zone	1024		7.70	120	194.6	210	20.7	374	681.6	187.9		1789	−8.44	−55.2	12.3	6.47
Jica 2	Sinai, S of the shear zone	1095		8.10	112.2	53.5	180	8.6	218	239	309		1120	−8.30	−52.7	14.2	5.44
Jica 4	Sinai, S of the shear zone	1125		8.00	112.2	53.5	132	16	218	365.7	200		1097	−7.19	−53.4	4.2	−2.68
El Hassana 2	Sinai, N of the shear zone	1241		8.00	348.7	102.1	545	53.5	1360	570	112		3091	−7.05	−50.2	6.2	−1.15
El Hassana 4	Sinai, N of the shear zone	1045		7.40	388.6	153.2	526	16.4	1346	955.2	98.9		3484	−7.46	−51.3	8.4	−3.63
Arif El Naga	Sinai, N of the shear zone	902		7.70	323.7	204.3	535	53.5	1251	1170	112.1		3650	−7.06	−52.4	4	−3.26
El Halal deep	Sinai, N of the shear zone	800		7.80	160.3	145.9	525	8.5	1034	340.1	329.8		2544	−6.22	−39.2	10.6	1.66
El Halal medium	Sinai, N of the shear zone	170		7.75	216.4	199.4	450	21.7	1225	662.4	197.9		2973	−6.04	−37.3	11	−4.29
Um Shihan	Sinai, N of the shear zone	903		7.90	561.1	354	607	17.9	1333	2218	118.7		5210	−6.42	−41.9	3.4	−1.02
El Bruk 1	Sinai, N of the shear zone	800		8.30	64.1	58.3	817	2	1240	54.7	399.3		2635	−9.53	−72.3	3.9	1.09
Bir El-Thamade	Sinai, N of the shear zone	1000		7.90	317	63	470	29	861	700	204		2644	−8.40	−58.2	9	−0.02
Ashalim 2a	Negev, N of the shear zone	710.13	35.4	6.80	213	93.25	1408	62.25	2277	611.4	315.75	6.6	4987	−7.2			−0.61
Ein Yorqeam 4	Arava, N of the shear zone	631.5	38.5	7.00	138	63.873	375	18	617	338	296.21	1.7	1848				−0.63
Ein Yorqeam 2a	Arava, N of the shear zone	715.305	37.2	7.16	151.1	61.1	395.7	25.6	667.1	376	302.2	1.54	1980	−6.49	−34.3	17.62	−1.85
Ein Yorqeam 3	Arava, N of the shear zone	695.73	36.2	6.99	222.4	79.6	465.9	28.9	893.4	506.6	340.5	1.86	2539	−6.36	−35.2	15.68	−3.32
Ein Yorqeam 1	Arava, N of the shear zone	683.35	38	6.90	159.1	67.2	435.9	26.7	751	421.1	324.5	1.58	2187	−6.41	−33.7	17.58	−3.13
Ein Yahav 6	Arava, N of the shear zone	821.5	40.3	6.92	225.3	95.4	273.3	26.3	613.7	513.1	270.2	2.26	2020	−7.26	−45.6	12.48	−1.18
Ein Ofarim 5	Arava, N of the shear zone	573.9	33.4	6.80	214.1	78.3	345.7	26.7	680.9	434.9	270.7	1.31	2053	−6.95	−40.8	14.8	0.25
Ein Ofarim 6	Arava, N of the shear zone		40.6	7.14	192.1	84.1	359	18.8	657	413.5	301.6	1.79	2028	−6.8	−40.3	14.1	0.82
Makhtesh Qatan 1	Arava, N of the shear zone	161.75	28.7	6.43	215.8	71.6	244.7	21.5	325.8	896.6	108.2	0.28	1884	−5.6	−32.1	12.7	−3.08
Makhtesh Qatan 3	Arava, N of the shear zone	640.45	37.7	7.00	151.8	61.9	454.5	28.6	758.1	410.3	317.4	1.84	2184	−6.59	−36.2	16.52	−2.84
Makhtesh Qatan 4	Arava, N of the shear zone	674.725	35	7.40	201.7	74.7	463.8	32.7	761.1	655.5	302.8	1.58	2494	−6.74	−40.1	13.82	−3.67
Paran 20	Arava, S of the shear zone	1415	54	7.01	281.4	90.4	312.2	36.8	749.1	577.4	225.7	3.833	2277	−7.83	−52.9	9.74	−1.15
Grofit 4	Arava, S of the shear zone	291.7	30.4	7.05	278	104.8	298.4	21.1	757.3	543.4	237.5	4.08	2245	−7.26	−48.4	9.68	−0.75
Qetura 5	Arava, S of the shear zone	358.5	33	7.01	226	88.4	225.6	15.5	601.7	369.5	248	2.88	1778	−6.6	−37.8	15	0.07
Shizafon 1	Arava, S of the shear zone	854.3	48.9	6.78	331.9	104.7	310.4	40.9	606.7	893.4	221.4	1.514	2511	−8.62	−58.5	10.46	0.5
Yaalon 3a	Arava, S of the shear zone		33.7	6.81	253.2	95	304.6	32.3	672.8	571.5	216.7	2.097	2148	−8.39	−58.2	8.92	0.16
Yaalon 6a	Arava, S of the shear zone	731.15	38.8	7.17	91	50.2	121.7	9.4	246.8	152.4	255.1	0.74	927	−5.73	−27.6	18.24	−0.37
Upper Cretaceous Calcareous aquifer																	
Maghara 1	North. Sinai				215	73	560	5	843	650	202		2548				0.73
Maghara 2	North. Sinai				117	78	400	5	557	550	183		1890				−0.63
Maghara 3	North. Sinai				439	207	1000	3	1685	1400	231		4965				1.26
Maghara 4	North. Sinai				94	50	225	3	351	200	283		1206				−0.09
Maghara 5	North. Sinai				234	107	540	6	929	1040	308		3164				−9.05
El Fateh A	North. Sinai			8.30	52.1	21.888	206.82	3.906	212.76	144.21	280.462	0.799	923	−4.41	−23.0	12.3	−0.38
El Fateh B	North. Sinai			8.40	150.3	68.096	448.11	11.718	602.82	576.84	152.425	1.598	2012	−5.63	−28.0	17	2.15
El Fateh C	North. Sinai			8.30	70.14	27.968	241.29	3.906	354.6	144.21	213.395	0.799	1056	−5.43	−28.0	15.4	−0.32
Qadesh Barnea.	North. Sinai				285.5	97.1	935	60.5	1471	888.8	292.6		4031				−0.24
Mashabim 1	Negev	550	34.9	6.88	170.9	85.8	563	19.5	992.1	407.4	283.6	2.45	2525	−5.47	−26.7		−0.63

(*continued on next page*)

Table 1 (*continued*)

Well_name	Area	Depth, m	Temperature, °C	pH	Ca, mg/l	Mg, mg/l	Na, mg/l	K, mg/l	Cl, mg/l	SO_4, mg/l	HCO_3, mg/l	Br, mg/l	TDS	$\delta^{18}O$	δD	*d*-Excess	RE
Mashabei Sade 1a	Negev		38.4	6.80	187	88.5	595	15.6	1026	418.6	783	2.9	3117	−5.80			−8.12
Nizana 1	Negev		37.9	6.40	256	116.5	1150	26.5	2017	602.7	278	4.7	4451	−6.00			−0.61
Nizana 3	Negev		37.6	6.40	230	116	1115	26	2010	525	327	4.9	4354	−5.90			−1.93
Revivim 2	Negev		41.4	6.40	175	84	650	17.5	1135	370	298	3.3	2733	−5.70			−0.25
Revivim 3	Negev	745	35.5	6.89	178.8	89.7	637.1	22.3	1187	455.9	287	3.87	2862	−5.49	−27.6		−3.32
Ashalim	Negev												3585				
Zeelim	Negev												2996				
Beer-Sheva 6	Negev												866				
Wadi Sheira 11	North. Sinai												1100				
El Hasana	North. Sinai												4120				
El Bruk 2	North. Sinai												5628				
Gafgafa	North. Sinai												3500				
Gebel Libni	North. Sinai												4500				
El Arish 15	North. Sinai												7000				

Well_name	rNa/rCl	rMg/rCl	rMg/rCa	rNa/rK	Q	rSO_4/rCl	$rSO_4/rHCO_3$	rCa/rSO_4	rCa/rCl	rCa/rNa	rMg/rNa	Cl/Br	$SI_{Calcite}$	$SI_{Dolomite}$	$SI_{Aragonite}$	SI_{Gypsum}	$SI_{Anhydrite}$
Kurnub Group aquifer																	
Jica 3	0.70	0.93	1.07	10.75	0.51	0.85	1.00	1.03	0.87	0.81	1.34		0.85	2.01	0.72	−1.64	−1.72
Jica 1	1.09	1.33	1.41	15.31	0.35	2.11	3.62	0.45	0.94	0.74	1.22		1.11	2.61	0.98	−1.00	−1.07
Jica 6	0.76	0.70	1.43	34.29	0.48	0.81	3.89	0.60	0.49	0.55	0.91		0.96	2.30	0.82	−0.97	−1.10
Wadi Sheira	0.70	0.37	0.80	18.94	0.88	0.14	0.35	3.36	0.46	0.32	0.53		1.14	2.45	1.01	−1.91	−2.05
Nekhel deep	0.95	0.64	0.85	16.85	0.51	1.10	3.06	0.68	0.75	0.41	0.68	444	1.09	2.35	0.96	−0.91	−0.99
Sudr El Heitan	0.87	1.52	2.67	17.25	0.35	1.35	4.61	0.42	0.57	1.06	1.75		0.61	1.90	0.48	−1.01	−1.08
Jica 2	1.27	0.72	0.79	35.60	0.56	0.81	0.98	1.13	0.91	0.34	0.56		1.27	2.72	1.15	−1.28	−1.35
Jica 4	0.93	0.72	0.79	14.03	0.51	1.24	2.32	0.74	0.91	0.46	0.77		0.99	2.13	0.86	−1.10	−1.17
El Hassana 2	0.62	0.22	0.48	17.32	1.27	0.31	6.47	1.47	0.45	0.21	0.35		1.07	2.09	0.94	−0.69	−0.76
El Hassana 4	0.60	0.33	0.65	54.55	0.90	0.52	12.27	0.98	0.51	0.33	0.55		0.45	0.97	0.32	−0.49	−0.56
Arif El Naga	0.66	0.48	1.04	17.01	0.62	0.69	13.26	0.66	0.46	0.44	0.72		0.68	1.63	0.55	−0.51	−0.59
El Halal deep	0.78	0.41	1.50	105.04	0.64	0.24	1.31	1.13	0.27	0.32	0.53		1.04	2.54	0.91	−1.20	−1.29
El Halal medium	0.57	0.47	1.52	35.27	0.63	0.40	4.25	0.78	0.31	0.51	0.84		0.60	1.53	0.46	−0.82	−1.03
Um Shihan	0.70	0.77	1.04	57.67	0.58	1.23	23.74	0.61	0.74	0.67	1.10		1.01	2.28	0.89	−0.15	−0.24
El Bruk 1	1.02	0.14	1.50	694.72	0.42	0.03	0.17	2.81	0.09	0.08	0.13		1.22	2.94	1.09	−2.28	−2.37
Bir El-Thamade	0.84	0.21	0.33	27.56	0.88	0.60	4.36	1.09	0.65	0.15	0.25		1.10	1.95	0.97	−0.59	−0.73
Ashalim 2a	0.95	0.12	0.72	38.47	0.59	0.20	2.46	0.84	0.17	0.08	0.13		−0.06	−0.04	−0.20	−0.92	−1.09
Ein Yorqeam 4	0.94	0.30	0.76	35.43	0.58	0.40	1.45	0.98	0.40	0.20	0.32	363	0.10	0.33	−0.03	−1.13	−1.28
Ein Yorqeam 2a	0.91	0.27	0.67	26.29	0.59	0.42	1.58	0.96	0.40	0.18	0.29	433	0.28	0.62	0.15	−1.06	−1.22
Ein Yorqeam 3	0.80	0.26	0.59	27.42	0.69	0.42	1.89	1.05	0.44	0.20	0.32	480	0.27	0.54	0.14	−0.85	−1.01
Ein Yorqeam 1	0.90	0.26	0.70	27.76	0.56	0.41	1.65	0.91	0.37	0.18	0.29	475	0.07	0.22	−0.06	−1.01	−1.17
Ein Yahav 6	0.69	0.45	0.70	17.67	0.74	0.62	2.41	1.05	0.65	0.40	0.66	272	0.18	0.45	0.05	−0.82	−0.95
Ein Ofarim 5	0.78	0.34	0.60	22.02	0.79	0.47	2.04	1.18	0.56	0.26	0.43	520	−0.04	−0.09	−0.17	−0.88	−1.06
Ein Ofarim 6	0.84	0.37	0.72	32.48	0.71	0.46	1.74	1.11	0.52	0.27	0.44	367	0.39	0.89	0.26	−0.96	−1.09
Makhtesh Qatan 1	1.16	0.64	0.55	19.36	0.53	2.03	10.53	0.58	1.17	0.34	0.55	1164	−0.91	−1.92	−1.05	−0.58	−0.78
Makhtesh Qatan 3	0.92	0.24	0.67	27.03	0.55	0.40	1.64	0.89	0.35	0.16	0.26	412	0.14	0.34	0.00	−1.04	−1.19
Makhtesh Qatan 4	0.94	0.29	0.61	24.12	0.54	0.64	2.75	0.74	0.47	0.18	0.30	482	0.56	1.11	0.42	−0.78	−0.95
Paran 20	0.64	0.35	0.53	14.43	0.89	0.57	3.25	1.17	0.66	0.33	0.55	195	0.43	0.84	0.31	−0.71	−0.74
Grofit 4	0.61	0.40	0.62	24.05	0.91	0.53	2.91	1.23	0.65	0.40	0.66	186	0.20	0.38	0.06	−0.73	−0.92
Qetura 5	0.58	0.43	0.64	24.75	0.96	0.45	1.89	1.47	0.66	0.45	0.74	209	0.17	0.36	0.03	−0.92	−1.10
Shizafon 1	0.79	0.50	0.52	12.91	0.75	1.09	5.13	0.89	0.97	0.39	0.64	401	0.16	0.28	0.04	−0.50	−0.57
Yaalon 3a	0.70	0.41	0.62	16.04	0.82	0.63	3.35	1.06	0.67	0.36	0.59	321	−0.07	−0.14	−0.21	−0.73	−0.91
Yaalon 6a	0.76	0.59	0.91	22.02	0.62	0.46	0.76	1.43	0.65	0.47	0.78	334	0.13	0.47	0.00	−1.50	−1.65

Upper Cretaceous Calcareous aquifer																	
Maghara 1	1.02	0.25	0.56	4.87	0.64	0.57	4.09	0.79	0.45	0.44	0.25		−0.12	−0.36	−0.26	−0.74	− 0.96
Maghara 2	1.11	0.41	1.10	3.48	0.40	0.73	3.82	0.51	0.37	0.34	0.37		−0.38	−0.60	−0.52	−1.00	− 1.22
Maghara 3	0.92	0.36	0.78	14.51	0.67	0.61	7.70	0.75	0.46	0.50	0.39		0.12	0.25	−0.03	−0.34	−0.56
Maghara 4	0.99	0.42	0.88	3.26	0.53	0.42	0.90	1.13	0.47	0.48	0.42		−0.19	−0.30	−0.33	−1.39	− 1.61
Maghara 5	0.90	0.34	0.75	3.92	0.44	0.83	4.29	0.54	0.45	0.50	0.37		0.04	0.08	−0.10	−0.58	−0.80
El Fateh A	1.50	0.30	0.67	2.30	0.35	0.50	0.65	0.87	0.43	0.29	0.20	266.28	0.87	1.71	0.72	−1.69	− 1.91
El Fateh B	1.15	0.33	0.75	1.66	0.52	0.71	4.81	0.62	0.44	0.38	0.29	377.23	0.99	1.98	0.85	−0.89	− 1.11
El Fateh C	1.05	0.23	0.66	2.69	0.54	0.30	0.86	1.17	0.35	0.33	0.22	443.80	0.86	1.67	0.72	−1.60	− 1.82
Qadesh Barnea. J.Ha	0.98	0.19	0.56	1.29	0.61	0.45	3.86	0.77	0.34	0.35	0.20		0.10	0.07	−0.05	−0.61	− 0.82
Mashabim 1	0.88	0.25	0.83	4.01	0.65	0.30	1.83	1.01	0.31	0.35	0.29	404.94	−0.03	0.07	−0.17	−1.04	− 1.21
Mashabei Sade 1a	0.89	0.25	0.78	5.01	0.43	0.30	0.68	1.07	0.32	0.36	0.28	353.79	0.38	0.89	0.24	−1.03	− 1.18
Nizana 1	0.88	0.17	0.75	2.95	0.75	0.22	2.76	1.02	0.23	0.26	0.19	429.15	−0.39	−0.67	−0.53	−0.85	−1.00
Nizana 3	0.86	0.17	0.83	3.00	0.70	0.19	2.04	1.05	0.20	0.24	0.20	410.20	−0.36	−0.57	−0.50	−0.94	−1.10
Revivim 2	0.88	0.22	0.79	4.46	0.69	0.24	1.58	1.13	0.27	0.31	0.24	343.94	−0.40	−0.65	−0.53	−1.09	−1.22
Revivim 3	0.83	0.22	0.83	3.51	0.63	0.28	2.02	0.94	0.27	0.32	0.27	306.72	−0.01	0.12	−0.14	−1.00	− 1.16

r = meq/l; concentrations in mg/l; ratios are given in meq/l with the exception of Cl/Br (weight ratios); RE = reaction error; SI = saturation index; Q = rCa/(rSO_4 + $rHCO_3$).

wards with another water body of heavier oxygen-isotope composition.

Chemical and isotopic similarity was also observed between the Kurnub waters north of the shear zone in Sinai and those occurring in the calcareous Upper Cretaceous Judea Group aquifer in the different parts of central and western Negev. Chemical analyses of groundwater hosted in the *calcareous Upper Cretaceous beds of central and northern Sinai* and in the Negev are based on data published by Abd Allatif and Galal (1997), Nada and Awad (1991) and Zaghloul (1999) and on information from the data bases of the Israel Hydrological Service. From several sources in Sinai only TDS-concentrations were published. The data (Table 1 and Fig. 7) indicate irregular distribution of salinities varying in a wide range starting with 1100 mg/l TDS in well Wadi Sheira 1 and reaching up to 7000 mg/l TDS in the wells near the El Maghara structure. The high TDS-concentrations in the groundwater north of the shear-zone in Sinai, continue into the Negev there they attain 4451 mg/l in the Nizana wells decreasing gradually northwards, towards the southern plunges of the Judea Mts. and reaching concentrations as low as 866 mg/l. The hydrogeological continuity between Sinai and the Negev is also supported by the semblance of the chemical characteristics. In *northern Sinai* the ionic assemblages are rNa > rCa > rMg and rCl > rSO_4 > $rHCO_3$. The water is characterized by a rather high pH of >8.3, by average rNa/rCl ~ 1, rMg/rCa of 0.74 and rSO_4 > rCa. The Cl/Br average weight ratio (362) is clearly higher than the marine value (286). $\delta^{18}O$ is in the $-5.63‰$ to $-4.41‰$ range and δD is between $-28‰$ and $-23‰$. In Sinai, close to- and north of the shear zone, groundwater from the Upper Cretaceous aquifer differs from groundwater from Kurnub aquifer only by higher Cl concentrations, lower rMg/rCa ratios (due to high Ca in the calcareous aquifer) and by a ''heavier'' isotopic signature. *In the western Negev*, the Cl content is in the range of 992–2061 mg/l, generally decreasing northwards. The average pH is lower (6.72) than in the northern Sinai. The ionic assemblage is identical to that of groundwater flowing in Upper Cretaceous beds (equivalent to Judea Group) in Sinai and so are the ionic ratios (rNa/rCl = 0.9, rMg/rCa = 0.76; rSO_4 > rCa and Cl/Br = 372). $\delta^{18}O$ is in the $-6.0‰$ to $-5.47‰$ range, (Fig. 9) and δD is between $-26.7‰$ and $-27.6‰$. The slight differences between the water of western Negev and those of Sinai can be attributed to the increasing influence of fresh water flowing in the limestone aquifer, from the Judea Mountains southwards into the study area.

The particular distribution of both salinities and chemical and isotopic compositions of groundwater together with their apparent coincidence with a major regional geological feature such as the shear zone, provoke several questions:

- Was or is there a common factor causing salinization of Kurnub groundwater north of the shear-zone in Sinai?
- Why did salinization not affect the same groundwater flowing in the same rock units south of the shear zone, in an area which is even more arid than northern Sinai and the Negev and much closer to the Rift with its particular salinization processes?
- Did the shear zone play an active role in the salinization process or was it just a geographical/morphological boundary?

Table 2 Peason's correlation matrix for chemical components of Kurnub-Group groundwater

	pH	rCa	rMg	rNa	rK	rCl	rSO_4	$rHCO_3$	$\delta^{18}O$
pH	1								
rCa	−0.248	1							
rMg	0.140	**0.779**	1						
rNa	−0.166	0.350	0.342	1					
rK	−0.439	0.490	0.154	0.437	1				
rCl	−0.116	0.578	0.553	**0.920**	0.500	1			
rSO_4	−0.106	**0.874**	**0.876**	0.301	0.338	0.444	1		
$rHCO_3$	−0.156	−0.527	−0.468	0.222	−0.212	−0.027	−0.566	1	
$\delta^{18}O$	−0.303	0.152	0.261	0.012	0.057	0.082	0.243	−0.113	1

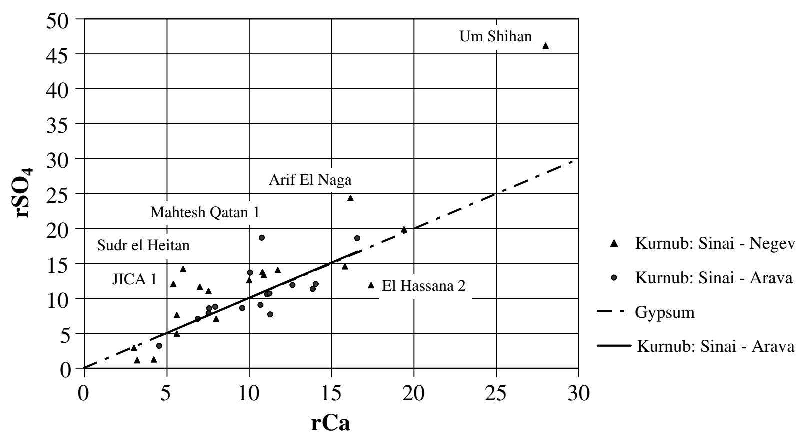

Figure 5 Evidence of gypsum dissolution from rCa—rSO_4 chart.

Hydrochemical modeling

The PHREEQC computer code (Parkhurst and Appelo, 1999) was employed for inverse hydrochemical modeling of both water/rock interaction and mixing processes along flow paths and for investigating the feasibility of various hydrogeological scenarios which could have occurred in central and northern Sinai and in the Negev to create the existing groundwater bodies. In all cases, groundwater from well Nekhel Deep in Sinai was taken as the fresh end-member, whereas the resultant brackish product was represented by groundwater from well Halal. The hydrochemical evolution of the Nekhel Deep water from rainwater was previously clarified (Rosenthal et al., 1998). The envisaged scenarios and their rationale are as follows:

1. *Nekhel Deep water evolving into Halal water exclusively by water/rock interaction without mixing with any other water body.* This scenario relates to a possible situation in which any ancient residual water was previously flushed out from the aquifer.
2. *Nekhel Deep water mixing with residual sea water*. This scenario envisages mixing of Nekhel Deep water with unflushed relics of proto-Mediterranean sea water, which penetrated inland during the Late Tertiary—Early Quaternary, mainly through erosive channels deeply incised into the Coastal Plain. This assumption was based on the findings of Rosenthal et al. (1998) and of Livshitz (1999).
3. *Nekhel Deep waters mixing with brines from Neogene beds such as encountered in borehole Afiq 1.* Borehole Afiq 1 was drilled in the immediate vicinity of the biggest erosive channel cutting through the Negev and penetrates into Lower Cretaceous beds. The brine encountered in the borehole might represent the saline waters which penetrated inland at the beginning of the Post-Messinian transgression (Rosenthal et al., 2006) and could occur as relics all through the investigated area.
4. *Nekhel Deep water mixing with deep-seated reduced brine encountered in lower Jurassic beds (Inmar Fm. in borehole Qeren 1).* It has been previously shown that groundwater salinization occurs close to and north of the shear zone. As indicated by geological cross-sections by Abd el Samie and Sadek (2001), Jenkins (1990) and Kashai et al. (1987), north of El Bruk 1, major displacements create geological conditions facilitating possible inter-aquifer flow between Jurassic, Lower Cretaceous and younger rock units. Such possible inter-aquifer flow might facilitate penetration of brines hosted in Jurassic rocks into Upper Cretaceous formations. Due to lack of published data from oil wells in Sinai and in order to investigate possible salinization by inflow of ancient

Table 3 Average chemical characteristics of Kurnub-Group aquifer in Sinai to the south (S) and to the north (N) from the Minsherah — Abu Kandu shear zone

Chemical characteristics	S	N	Ratio N/S
pH	8.06	7.84	
Ca, mg/l	111.03	297.49	2.68
Mg, mg/l	84.19	160.03	1.90
Na, mg/l	167.25	559.38	3.34
K, mg/l	14.71	25.31	1.72
Cl, mg/l	290.50	1206.25	4.15
SO_4, mg/l	394.45	833.8	2.11
HCO_3, mg/l	212.09	196.59	
$\delta^{18}O$, %	−7.76	−7.27	
δD, %	−53.19	−50.35	
d-excess, %	8.93	7.06	
rNa/rCl	0.91	0.72	0.79
rMg/rCl	0.87	0.38	0.44
rCa/rCl	0.74	0.44	0.60
rCa/rNa	0.59	0.34	0.58
Mg/Na	0.97	0.56	0.58
Mg/Ca	1.23	1.01	
Na/K	20.38	126.14	6.19
$Q = Ca/(SO_4 + HCO_3)$	0.52	0.74	1.43
SO_4/Cl	1.05	0.50	0.48
SO_4/HCO_3	2.48	8.23	3.32
Ca/SO_4	1.05	1.19	
SI_Calcite	1.00	0.90	
SI_Dolomite	2.31	1.99	
SI_Aragonite	0.87	0.77	
SI_Gypsum	−1.23	−0.84	
SI_Anhydrite	−1.32	−0.95	

All the ion ratios are ratios of equivalent concentrations SI is a saturation index.

brines, Nekhel Deep water was mixed with brine from the Lower Jurassic Inmar Formatiion in borehole Qeren 1 (located in southern Negev, close to the border with Sinai).

5. *Nekhel Deep water mixing with brackish groundwater encountered in Jurassic beds in the El Maghara structure (El Ramly, 1967; Abd Allatif and Galal, 1997)*. This groundwater is characterized by high sulfate concentrations (1270—1400 mg/l, $rSO_4/rCl = 0.36–0.61$), which could be caused by contact with numerous veins of anhydrite, which criss-cross the Jurassic section (Goldberg et al., 1971; Goldberg and Raab, 1987). Owing to direct recharge on the El Maghara structure, Jurassic groundwater might spread east- and southwards reaching the investigated flow path. Moreover, a deep-seated NEE striking fault connects between the two structures, El Maghara and El Halal (Jenkins, 1990), and could act as a preferential flow path for these waters facilitating their mixing with those from the Kurnub Group. Sulfate-rich Jurassic groundwater were also encountered in southern Israel (Mahtesh Qatan wells), where at Cl concentrations of 500—650 mg/l, rSO_4/rCl ratio is close to 2.
6. *Nekhel Deep water mixing with brine encountered in the lower-most portion of the Judea Group aquifer (Sadot oil wells)*. Owing to faulting in Sinai and the Northern Negev, Judea Group layers are often positioned against Kurnub Group layers (Abd el Samie and Sadek, 2001; Weinberger, 2003) facilitating lateral inter-aquifer flow.
7. *Nekhel Deep waters mixing with flood waters sampled in the El Arish area (northern Sinai)*. As indicated by numerous findings (Mualem, 1971; Movshovitz and Ben Zvi, 1973; El Ghazawi, 1992), in northern Sinai, groundwater replenished by flood waters and flowing in alluvial beds have high salinity. The model checks whether Nekhel Deep water is salinized along their flow paths northwards by the possible infiltration of such saline flood waters through permeable formations and percolating into the Kurnub-Group aquifer.

Model constraints

The chemical end-members considered in inverse modeling are given in Table 4. The speciation of groundwater from the Halal borehole in Sinai and from well Ashalim 2a in the Northern Negev by the PHREEQC program revealed that groundwater in the Kurnub-Group aquifer is saturated with respect to calcite and dolomite, and is strongly undersaturated with respect to solid sulfates and halite. Therefore, possible precipitation of calcite or dolomite and dissolution of anhydrite (or gypsum) and halite, were set as model constraints. These minerals are present both in the Cretaceous sedimentary rock-formations in Sinai and in the Messinian evaporites occurring in the Haruvit and Afiq-Gaza channels incised into the subsurface of the Coastal Plain (Fleischer, 1979). Pyrite encountered in Cretaceous rock in Sinai was assumed to be formed from goethite by reaction with H_2S produced through sulfate reduction by organic matter. Correspondingly, a possible sink for CH_2O and a CO_2 source were set. Since clay particles are always present, major-cation exchange (Ca^{2+}, Mg^{2+}, Na^+, K^+) was permitted. When estimating the plausibility of the generated models, the common assumption was accepted that models with very large mole transfers (>1 mol), are not realistic (Parkhurst, 1999). The available Cl/Br ratios and $\delta^{18}O$ values were used for validation of the plausible models. Final Cl^- and Br^- concentrations were calculated by using mixing fractions and mole transfers received for each model. Their ratio has been compared to the value estimated for the water from the Halal well. Br concentrations in groundwater from well Halal had not been reported in literature. However, by considering the chemical semblance of this groundwater with that from wells Ashalim 2a and Ein Yorkeam in the Northern Negev (located on the studied flowpath), a range of possible Cl/Br ratios for Halal groundwater was estimated as 328—406 which is higher than in seawater, but lower than in the Nekhel Deep-deep groundwater (444). The error of the Cl/Br ratio was estimated by using reference standard deviations (RSD) of Cl^- and Br^- determination in brackish groundwater by modern equipment. The error estimations are of 2% and 5% respectively. Hence, the error of the Cl/Br ratio will equal the sum of the RSD, i.e. of about 7%.

All modeled cases considered processes of mixing of deep seated water bodies which could not be subjected to evaporation after their deep confinement. Under such conditions evaporative fractionation of oxygen isotopes was impossible. Fractionation due to water—rock interaction at relatively low mass transfers (as shown by modeling)

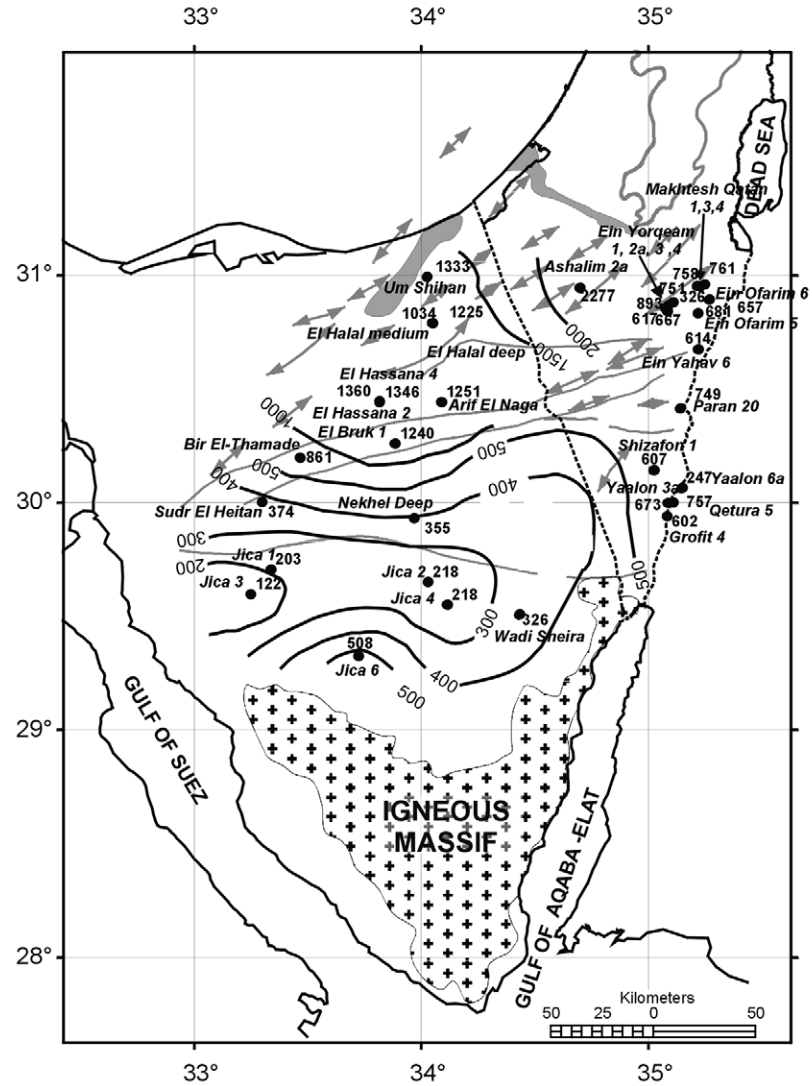

Figure 6 Chloride concentrations (mg/l) in groundwater hosted in the Kurnub Group aquifer.

should be insignificant. Therefore, oxygen isotopes could be considered as conservative and used for the validation of the received models.

The average $\delta^{18}O$ in Kurnub Group groundwater north of the shear zone ($-7.45‰$) (Fig. 9) is slightly heavier than south of this zone ($-7.70‰$) hinting to possible mixing with heavier water such as seawater, brine or flood water entering the system north of the shear zone. To some degree, the heavier isotope signature may also be a result of isotope exchange between oxygen of the water and the oxygen of the carbonate fraction (Ayalon and Longstaffe, 1988) occurring in the rocks of the Kurnub Group, which increases north of the shear zone (Kroitoru, 1980).

Results of modeling

The acceptable resultant models are summarized in Table 5. All models are characterized by small amount of precipitating carbonates (calcite or dolomite — 0.001—0.009% of the rock mass), by formation of pyrite (0.001—0.006% of the rock mass), consumption of organic matter (0.001—0.006% of the rock mass) with corresponding formation of CO_2 (0.0006—0.0069 mol/l) and by cation exchange accompanied by increase in Mg^{2+} (and sometimes in Ca^{2+}) in groundwater and by impoverishment in Na^+ and K^+. Dissolution of anhydrite and/or of halite was encountered only in a few of the models.

Discussion of modeling results

1. A single model was found describing direct transformation of Nekhel Deep groundwater to that encountered in the Halal well. The transformation was exclusively by water—rock interaction (without mixing with any other water body), by dissolving both halite and anhydrite. In the resultant groundwater, dissolution of halite generated a very high ratio of calculated Cl^- and Br^- concentrations (Cl/Br = 1347) i.e. a very high ratio value which does not match with the ratio expected in well El Halal Deep (328 ± 23 to 406 ± 28).

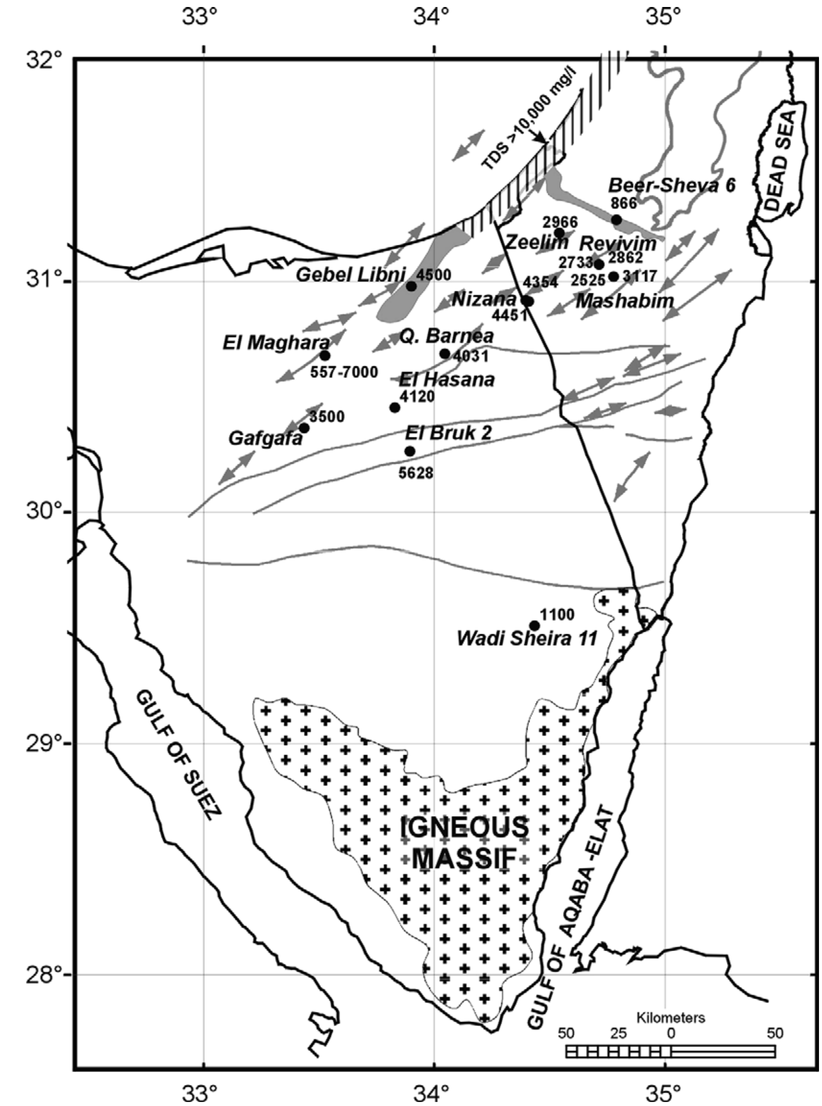

Figure 7 TDS concentrations (mg/l) in groundwater hosted in the calcareous Upper Cretaceous aquifer in Sinai and in the Negev.

2. All three models describing mixing of Nekhel Deep groundwater with residual seawater have similar features. They indicate a small mixing portion of seawater (about 3.3%) and the absence of additional dissolution of halite. This leads to both preserving the Cl/Br ratio (325) close to the lower limit of the plausible interval (328 ± 23 to 406 ± 28) and to heavier oxygen isotope values. Only one of the models indicated limited dissolution of calcium sulfate (about 0.003% of the rock mass).
3. Two models described the mixing of Nekhel Deep groundwater with a small portion (1.8%) of the Afiq-1 brine, which represents water from the Neogene erosive channels. These models are characterized by absence of halite and anhydrite dissolution. The ratio of calculated Cl^- and Br^- concentrations in the resultant groundwater (Cl/Br = 486) is higher than in both Nekhel Deep groundwater (444 ± 31) and in groundwater occurring north of the shear zone (328 ± 23 to 406 ± 28).
4. Four mixing models were developed for Nekhel Deep groundwater with the Lower-Jurassic brine such as encountered in borehole Qeren 1. Only in one model the ratio of calculated Cl^- and Br^- concentrations in the resultant groundwater (Cl/Br = 321) was found to be close to the expected Cl/Br range (328 ± 23 to 406 ± 28). All other models show highly divergent values such as 457 and 157. The model, which is plausible from a point of view of the Cl/Br ratio, is characterized by mixing with a very small fraction of brine (0.32%) and by minor dissolution of halite (0.008% of the rock mass) and by no dissolution of calcium sulfates.
5. Three models evolved for the possible mixing of Nekhel Deep groundwater with Lower-Jurassic brackish sulfate-rich groundwater as encountered in the boreholes of El Maghara (El Ramly, 1967). The models involve a relatively high portion of the Jurassic groundwater (31.8%) mixing with Kurnub Group water. Only one of the models involves dissolution of anhydrite (0.007% of the rock mass). The rNa/rCl ratio in El Maghara groundwater is >1 (1.2) indicating possible dissolution of evaporates. Therefore, Cl/Br ratio in this water should exceed the marine value of 286). At an assumed Cl/Br values of 305—400 for El Maghara groundwater, the ratio of calcu-

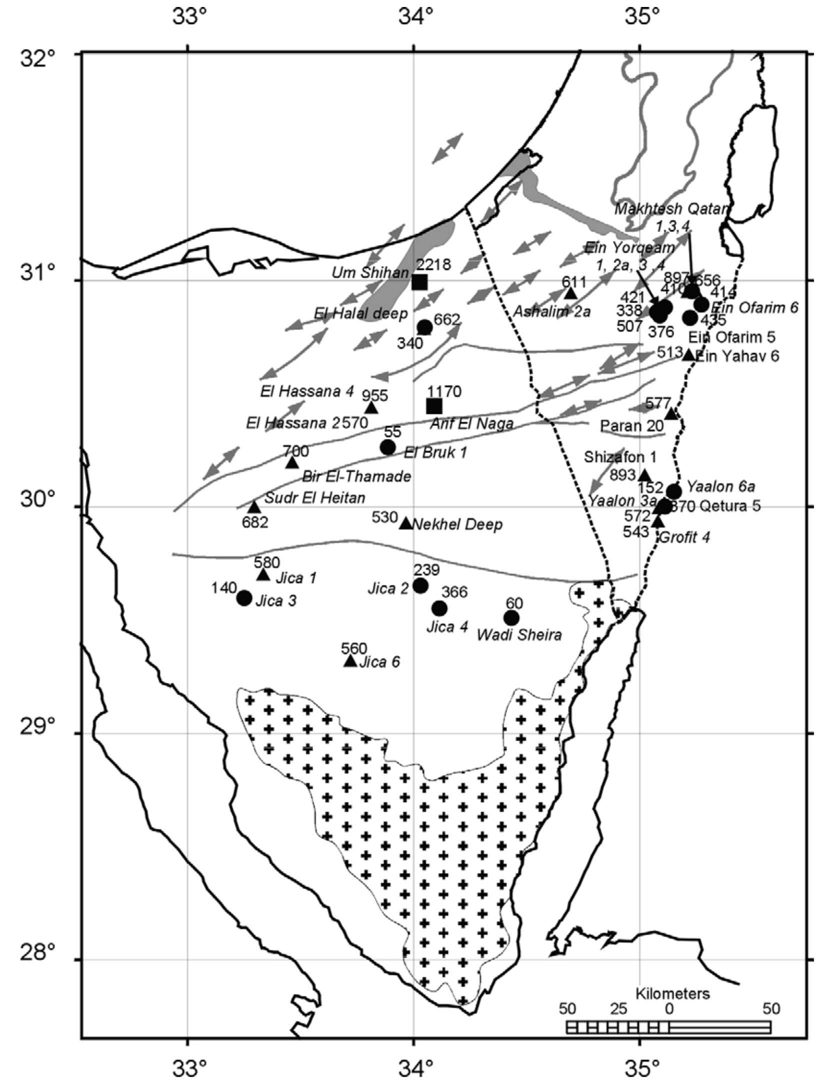

Figure 8 Sulfate concentrations (mg/l) in groundwater hosted in the Kurnub Group aquifer: ●, <500 mg/l; ▲, >500 mg/l; ■, >1000 mg/l.

lated Cl^- and Br^- concentrations in the resultant groundwater was found to be within a range of the expected Cl^-/Br^- values (328 ± 23 to 406 ± 28).

6. Two models evolved for mixing of Nekhel Deep groundwater with Upper Jurassic brackish sulfate-rich groundwater of the same El Maghara site (Abd Allatif and Galal, 1997). They are characterized by relatively high mixing fraction (about 52%) of Upper Jurassic groundwater, absence of both halite and anhydrite dissolution and the ratio of calculated Cl^- and Br^- concentrations in the resultant groundwater within a range of the expected Cl^-/Br^- values (328 ± 23 to 406 ± 28).
7. Five mixing models of Nekhel Deep groundwater with reduced brine encountered in the lowermost portions of the Judea Group aquifer (Sadot oil wells) are characterized by the complete absence of calcium sulfate dissolution and by very low ratios of calculated Cl^- and Br^- concentrations in the resultant groundwater (239—245) and are therefore not plausible.
8. Two mixing models of Nekhel Deep groundwater with flood water, sampled in the El Arish area (northern Sinai), were found. These models are characterized by no dissolution of halite and of anhydrite. As there are no data for Br^- concentrations in El Arish groundwater, it was not possible to validate the evolved models. Moreover, these models indicate that the portions of flood water in the mixing reactions are high, i.e. about 42% (Table 5). There are no published data on the $\delta^{18}O$ content in flood water in Sinai. However, such measurements were carried out in the Arava Valley (which is also a hyper-arid zone) and are in the $-5.3‰$ to $1.0‰$ range (Anker, 2001). These figures are considerably heavier than values characterizing Kurnub Group paleowater. Therefore, massive addition of flood water is incompatible with the ''light'' isotopic signature of Hallal 1 groundwater, and therefore models involving massive contribution of flood water are not plausible (see Fig. 10).

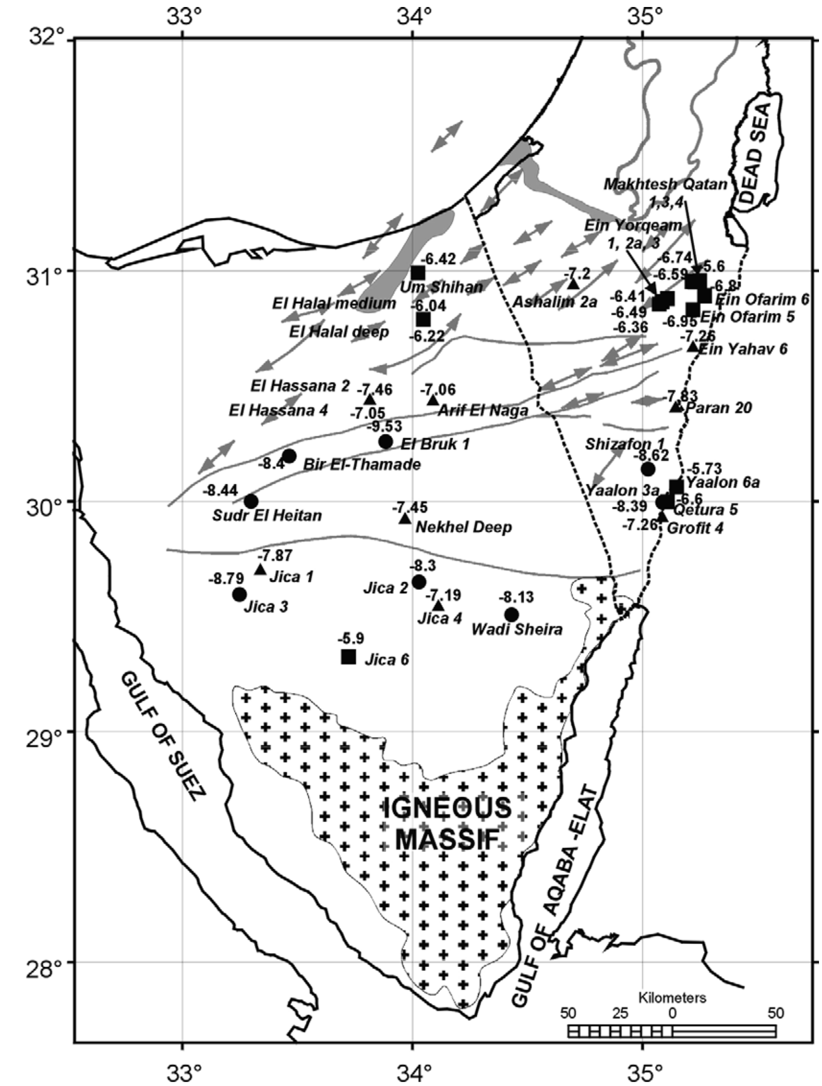

Figure 9 $\delta^{18}O$ in groundwater hosted in the Kurnub Group aquifer: ■, <−6.0‰; ▲, <−7‰; ●, < −8‰. Data from Abd el Samie and Sadek (2001), Abd Allatif and Galal (1997), Fekry (2001) and Nada and Awad (1991) and from databases of the Mekorot Co., Tel Aviv and the Hydrological Service of Israel, Jerusalem.

In view of the modeling results and considering both the necessary dissolution of anhydrite (proved by good $Ca^{2+}-SO_4^{2-}$ correlation in groundwater) and the ratios of reconstructed Cl and Br concentrations, the transformation of Nekhel fresh groundwater into El-Halal brackish groundwater could be only explained by mixing of Nakhel water either with residual seawater or with brackish Lower Jurassic groundwater of El Maghara type. Actually, both scenarios could occur simultaneously.

The chemical composition of Kurnub Group groundwater encountered along the flow path from northern Sinai to the Negev Highlands and further to the Dead Sea differs significantly from that encountered in the Halal well. Between northern Sinai and the Yorqeam wells in the Negev Highlands, Kurnub Group groundwater flows under conditions of deep confinement, completely isolated from any contemporary recharge. The difference in ionic concentrations between the water in northern Sinai and Yorqeam indicates that the latter has a much higher Cl content, whereas the concentration of SO_4 decreases. The previous PHREEQC modeling (Rosenthal et al., 1998) showed that the water of Yorqeam could be derived from that of Sinai mainly by dissolution of halite, plagioclase, organic matter and goethite and by precipitation of calcite, Ca-smectite, silica and pyrite. Finally, the chemical composition of Kurnub Group groundwater encountered in wells located close to the Dead Sea evolved as the result of mixing of the Kurnub groundwater encountered in the Yorqeam wells in the Negev Highlands with typical Ca—Cl water of the Rift. The PHREEQC modeling revealed that the mixing process (with a very small amount of brine) was accompanied by dissolution of dolomite, gypsum, halite, outgasing of CO_2 and the precipitation of calcite and K-smectite. The dissolving halite and gypsum were most likely residuals from higher levels of the proto Dead Sea (Rosenthal et al., 1998).

Table 4 Chemical characteristics of endmembers used for PHREEQC inverse modeling

Water	Ca mmol/l	Mg mmol/l	Na mmol/l	K mmol/l	Cl mmol/l	SO_4 mmol/l	HCO_3 mmol/l	Br mg/l	Cl/Br	$\delta^{18}O$, %
Nekhl Deep 1, Rosenthal et al., 1998 – INITIAL	3.768	3.207	9.482	0.563	10.011	5.518	3.605	0.8	444	−8.23
El Halal Deep, Abd el Samie and Sadek, 2001 – FINAL	4.000	5.999	22.836	0.217	29.160	3.540	5.405		328–406[*]	−6.22
Average Mediterranean seawater (Zilberbrand et al., 2005)	12.256	58.95	522.51	11.434	629.75	28.608	2.746	71.2	312	+1.90
Afiq 1, 1196–1210 m, Cretaceous (Yakhini Formation)	59.5	25.5	977	5	1066	32	10	74	512	+3.0
Qeren 1, 2919–2935 m, L. Jurassic (Inmar Formation)	388.48	86.1	1856.29	27.62	2809.6	5.255	2.39	816	122	−0.96
El Maghara, Lower Jurassic (El Ramly, 1967)	3.393	4.937	88.034		73.337	13.22	4.917			
El Maghara, Upper Jurassic (Abd Allatif and Galal, 1997)	10.954	8.517	43.498	0.077	47.528	14.574	3.819			
Sadot 2, Cretaceous (Yagur Formation)	2	1.5	391	2.5	397	0.5	12	64	220	+3.21
El Arish shallow aquifer, T80b (Mualem, 1971)	6.313	7.529	46.977	0.384	56.695	6.558	3.458			−5.3% to 1.0%[**]

[*] 328 mg/l – in Ashslim 2a well, 406 mg/l – in Ein Yorqeam well.
[**] by Anker (2001) for the Arava.

Table 5 Results of PHREEQC inverse modeling and calculation of the synthetic Cl/Br ratio

Model	Mixing fraction		Mole transfers, mol/kgw												Calculation results		
	Soln 1	Soln 2	Anhydrite	Halite	Calcite	Dolomite	Goethite	Pyrite	CH_2O	CO_2 (g)	CaX_2	MgX_2	NaX	KX	Cl, mg/l	Br, mg/l	Cl/Br ratio
Nekhl + 0	1.000	0.000	0.0014	0.0204	0	−0.0011	0.0016	−0.0016	0.0060	−0.0018	0	0.0039	−0.0075	−0.0003	1078	0.80	1347
Nekhl + seawater	0.967	0.033	**0.0016**	0	0	−0.0016	0.0021	−0.0021	0.0078	−0.0026	0	0.0026	−0.0044	−0.0007	1082	3.33	**325**
Nekhl + seawater	0.967	0.033	0	0	0	−0.0008	0.0013	−0.0013	0.0049	−0.0012	0.0008	0.0018	−0.0044	−0.0007	1082	3.33	325
Nekhl + seawater	0.967	0.033	0	0	−0.0017	0	0.0013	−0.0013	0.0049	−0.0012	0.0016	0.0009	−0.0044	−0.0007	1082	3.33	325
Nekhl + Afiq	0.982	0.018	0	0	−0.0015	0	0.0012	−0.0012	0.0044	−0.0011	0.0007	0.0024	−0.0056	−0.0004	1044	2.15	486
Nekhl + Afiq	0.982	0.018	0	0	0	−0.0008	0.0012	−0.0012	0.0045	−0.0012	0	0.0032	−0.0059	−0.0004	1031	2.12	486
Nekhl + Qeren 1 (LJ)	0.998	0.002	0	0.0154	0	−0.0005	0.0009	−0.0009	0.0034	−0.0006	0	0.0031	−0.0058	−0.0004	1093	2.39	457
Nekhl + Qeren 1 (LJ)	0.992	0.008	0	0	0	−0.0004	0.0009	−0.0009	0.0034	−0.0006	−0.0022	0.0025	0	−0.0005	1146	7.30	157
Nekhl + Qeren 1 (LJ)	0.992	0.008	0	0	−0.0009	0	0.0009	−0.0009	0.0034	−0.0006	−0.0018	0.0021	0	−0.0005	1146	7.30	157
Nekhl + Qeren 1 (LJ)	0.997	0.003	0	0.0121	−0.0009	0	0.0009	−0.0009	0.0034	−0.0006	0	0.0026	−0.0047	−0.0004	1103	3.43	321
Nekhl + El Maghara (LJ)	0.682	0.318	0	0	0	−0.0018	0.0022	−0.0022	0.0081	−0.0031	0.0022	0.0041	−0.0123	−0.0002	1069	3.26	328
Nekhl + El Maghara (LJ)	0.682	0.318	**0.0043**	0	0	−0.0040	0.0043	−0.0043	0.0163	−0.0069	0	0.0062	−0.0123	−0.0002	1069	3.26	**328**
Nekhl + El Maghara (LJ)	0.682	0.318	0	0	−0.0036	0	0.0022	−0.0022	0.0081	−0.0031	0.0040	0.0022	−0.0123	−0.0002	1069	3.26	328
Nekhl + El Maghara (UJ)	0.475	0.524	0	0	−0.0058	0	0.0033	−0.0033	0.0125	−0.0049	0.0023	0	−0.0045	−0.0001	1052	3.23	**326**
Nekhl + El Maghara (UJ)	0.483	0.517	0	0	0	−0.0029	0.0033	−0.0033	0.0124	−0.0048	−0.0006	0.0029	−0.0045	−0.0001	1042	3.19	**326**
Nekhl + Sadot 2 (UC)	0.946	0.054	0	0	0	−0.0004	0.0008	−0.0008	0.0029	−0.0008	0.0008	0.0033	−0.0077	−0.0005	1094	4.58	239
Nekhl + Sadot 2 (UC)	0.946	0.054	0.0015	0	0	−0.0012	0.0015	−0.0015	0.0058	−0.0021	0	0.0041	−0.0077	−0.0005	1094	4.58	239
Nekhl + Sadot 2 (UC)	0.946	0.054	0	0	−0.0009	0	0.0008	−0.0008	0.0029	−0.0008	0.0012	0.0029	−0.0077	−0.0005	1094	4.58	239
Nekhl + El Arish	0.583	0.417	0	0	−0.0011	0	0.0011	−0.0011	0.0040	−0.0010	0	0.0010	−0.0017	−0.0003	1044	2.57	406
Nekhl + El Arish	0.583	0.417	0	0	0	−0.0008	0.0012	−0.0012	0.0046	−0.0014	0	0.0017	−0.0032	−0.0003	1045	2.57	406

Negative mole transfer is connected with either precipitation, or gas formation, or impoverishment of solution by cation exchange. Positive mole transfer is connected with either dissolution, or enrichment of solution by cation exchange. LJ, UJ, UC — groundwater from Lower Jurassic, Upper Jurassic and Upper Cretaceous aquifers, respectively.

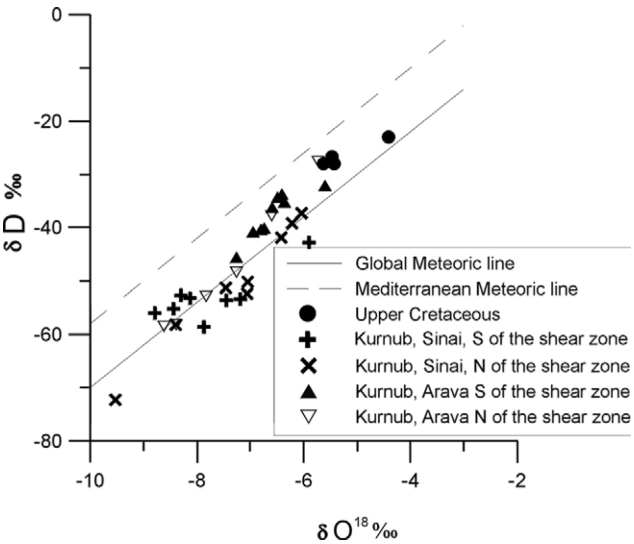

Figure 10 The $\delta D - \delta^{18}O$ relationships in groundwater.

Conclusions

The present study reveals that the shear zone cutting through central Sinai and western Negev plays an important role in the salinization of Kurnub_Group paleowaters flowing northeastwards to the Negev. Inverse hydrogeochemical modeling indicates that the main sources for salinity increase in the shear zone and in adjacent areas could be due to two different sources. One such salinization factor could be sulfate-rich brackish groundwater occurring in Lower or Upper Jurassic formations, which are in fault-controlled lateral contact with Kurnub Group rocks. According to Goldberg and Raab (1987), the thick Jurassic section contains a major amount of secondary anhydrite occurring in veins. Considering the absence of anhydrite in the Triassic beds of Sinai (Druckman, 1987), its origin could be in the Jurassic of the Halal region as well as in the thick beds of this evaporite mineral occurring in the Upper Triassic Ramon Group in the Arif el Naga area, in the Ramon saddle and further east- and northeastwards in the Negev and in Jordan (Rosenthal et al., 2005). These authors also reported massive occurrence of sulfate-rich brines in the Negev in the Ramon and Arad Groups (Upper Triassic and Jurassic — particularly in Lower Jurassic). Another plausible source of salinity could be unflushed seawater in the subsurface of northern Sinai and western Negev. According to Rosenthal et al. (1999) the post-Messinian (Lower Pliocene) transgression penetrated inland (into northern Sinai, the western Negev and into the Coastal Plain of Israel) both through erosional channels, which were incised during the Neogene, and inundating outcrops of permeable formations (Zilberbrand et al., 2005). In view of the absence of halite dissolution (as indicated by the models — Table 5), it is plausible that in the studied areas seawater could have penetrated inland through the upper parts of the channels which are rich in beds of gypsum, but contain no halite (Fleischer, 1979).

The brackish groundwater in Upper Cretaceous aquiferous beds in northern Sinai and in the Negev (Judea Group), seem to originate from the Kurnub Group. Due to the absence of impermeable strata between the Upper and the Lower Cretaceous and also as the result of faulting, Kurnub Group waters may flow unimpeded into Upper Cretaceous beds. The higher salinity of waters in the Upper Cretaceous beds could be caused by mixing with unflushed relics of seawater. The heavier isotopic signature of the groundwater in wells located close to the El Maghara structure in Sinai and in the Beer Sheva area (Israel) is due to mixing with local, modern recharge water.

The coincidence between the shear zone and groundwater salinization phenomena cannot be incidental. On one hand, this is a zone of intensive faulting, which could provide preferential flow paths for the sulfate-rich brackish water originating in the Jurassic and possibly older formations and penetrating laterally into downfaulted Cretaceous beds. On the other hand, the major morphotectonic feature of the shear zone, that extends northeastwards into the Negev to the Ramon saddle, could have created a huge obstacle, which prevented penetration of the invading seawater further inland. This could possibly be a reason for the fact that south of this morphotectonic feature, in areas, which are even more arid than northern Sinai and the Negev and much closer to the Rift (with its particular salinization processes), no such salinization phenomena could be identified.

Acknowledgements

We are grateful to Dr. Y. Bartov of Ministry of National Infrastructure of Israel, to Dr. Y. Guttman of Mekorot Company and to reviewers of the Journal for their help and valuable remarks. We are highly indebted to our colleague Dr. M. Weiss from the Hydrological Service of Israel for critical reading of the manuscript and improving its style.

References

Abd Allatif, T.A., Galal, G.H., 1997. Groundwater detection in fractured limestone: El Maghara, Sinai as case study. Desert Inst. Bull. Egypt 47 (1), 15—30.

Abd el Rahman, H., 2001. Evaluation of groundwater resources in Lower Cretaceous aquifer system in Sinai. Water Resour. Manage. 15, 187—202.

Abd el Samie, S.G., Sadek, M.A., 2001. Groundwater recharge and flow in the Lower Cretaceous Nubian sandstone aquifer in the Sinai Peninsula using isotopic techniques and hydrochemistry. Hydrogeol. J. 9, 378—389.

Anker, Y., 2001. Evolution of the carbonate system in hyper arid environment — Central Arava area, Israel and its implications for ^{14}C-dating. M.Sc. Thesis, Hebrew University, Jerusalem (in Hebrew, English Abstract).

Arad, A., 1964. The geology and hydrogeology of the Lower Cretaceous in the southern Negev and in the Judea Mountains. Ph.D. Thesis, Hebrew University, Jerusalem (in Hebrew, English abstact).

Arad, A., Kafri, U., 1980. Hydrogeological inter-relationship between the Judea Group and the Nubian sandstone aquifers in Sinai and in the Negev. Israel J. Earth Sci. 29, 67—72.

Ayalon, A., Longstaffe, F.J., 1988. Oxygen isotope studies of diagenesis and pore-water evolution in the Western Canada sedimentary basin; evidence from the Upper Cretaceous basal

Belly River sandstone, Alberta. J. Sediment. Res. 58 (3), 489—505.

Baida, U., Goldschtoff, Y., Kidron, I., 1978. A numerical model of the Cenomanian of the southern part of the Yarkon-Taninim basin. Tahal, Tel Aviv, Rep. 01/78/08 (in Hebrew), 45 pp.

Bar Joseph, J., 1978. The Neogene erosive channel, Gaza—Beer Sheva area: a possible outlet for groundwater of the Cenomanian aquifer in Beer Sheva Basin. (In Hebrew). Tel Aviv, Tahal, 8 P. {01/78/30}.

Bartov, Y., 1974. A structural and paleogeographical study of the central Sinai faults and domes. Ph. D. Thesis, Hebrew University, Jerusalem (in Hebrew, English abstract).

Bartov, Y., Arkin, Y., Lewy, Z., Mimran, Y., 1981. Regional stratigraphy of Israel — a guide for geological mapping. Geological Survey of Israel, 32pp.

Druckman, Y., 1987. Triassic rock-units in Sinai — transitionary phenomena from continental to marine environments. In: Gvirtzman, G., Shmueli, A., Gross, Y., Ben Arieh, Y., Harel, M. (Eds.), Sinai, Part 1 — Physical Geography. Ministry of Defense and Ha'Aretz Publ. House, pp. 59—70.

El Ghazawi, M.M., 1992. Hydrogeologic evaluation of the groundwater withdrawals in El Sheikh Zuwayid-Rafah coastal area, northeast Sinai, Egypt. Egypt J. Geology 36 (1—2), 1—16.

El Ramly, I.M., 1967. Contribution to the hydrogeological study of limestone terrains in U.A.R. In: Proc. of International Symposium on Hydrology of Fractured Rocks, Dubrovnik, Yugoslavia, IAH Publ. 73, v. 1: 348—377pp.

Eyal, M., Bartov, Y., Shimron, A.E., Bentor, Y.K., 1980. Sinai-Geological Map, scale 1:500,000. Israeli Geological Survey, Tel Aviv.

Eyal, M., Bartov, Y., Shimron, A.E., Bentor, Y.K., 1987. Explanatory notes to geological photo map scale 1:500,000. In: Gvirtzman, G., Shmueli, A., Gross, Y., Ben Arieh, Y., Harel, M. (Eds.), Sinai Part 1 — Physical Geography. Ministry of Defense and Ha'Aretz Publ. House, pp. 21—42.

Fekry, A.M., 2001. Hydrogeological aspects of the carbonate aquifer system in Sinai and the identification of promising areas for groundwater development. The 6th Gulf Water Conference, Ryadh, Kingdom of Saudi Arabia, pp. 1—13.

Fleischer, L., 1979. Geological investigations for oil prospection in the Mediterranean Sea. Rep.79/31 Oil Exploration (Investments) Ltd., 78pp.

Fleischer, L., Gelberman, E., Wolff, O., 1993. A geological—geophysical reassessment of the Judea Group (Yarqon-Taninim aquifer). The Institute for Petroleum Research and Geophysics, Job Report 244/147/92, 91pp.

Goldberg, M., Raab, M., 1987. Observations and elucidations on the Jurassic at Gebel El Maghara—North Sinai (General and economical aspects and bearings on the Jurassic in Israel). In: Gvirtzman, G., Shmueli, A., Gross, Y., Ben Arieh, Y., Harel, M. (Eds.), Sinai, Part 1 — Physical Geography. Ministry of Defense and Ha'Aretz Publ. House, pp. 71—84.

Goldberg, M., Barzel, A., Mimran, Y., Cook, P., 1971. The Jurassic section in Gebel El Maghara, North Sinai with a projection to the neighbouring regions. Isr. Geol. Soc. Annual Meeting, Northern Sinai, pp. 9—12.

Gvirtzman, H., 2002. Water Resources of Israel — Chapters in Hydrology and Environmental Sciences. Yad Ben Zvi Press, Jerusalem, pp. 287 (in Hebrew).

Gvirtzman, G., Buchbinder, B., 1977. The dessication events in the eastern Mediterranean during Messinian times as compared with other Miocene dessication events around the Mediterranean. Technip, Paris, pp. 411—420.

Hening, S., Vengosh, A., Ganor, J., Weyhenmeyer, C.E., Mayer, B., Sturchio, N.C., Bullen, T.D., Paytan, A., 2005. New isotope evidences for the origin groundwater from the Nubian sandstone (Kurnub Group) in the Negev. Israel Geological Society, Annual meeting in Mashabim, p. 47.

Issar, A., 1981. The rate of flushing as a major factor in deciding the chemistry of water in fossil aquifers in southern Israel. J. Hydrol. 54, 285—295.

Issar, A., Bein, A., Michaeli, A., 1972. On the ancient water of the Upper Nubian Sandstone aquifer in central Sinai and southern Israel. J. Hydrol. 17, 353—374.

Jenkins, D.A., 1990. North and Central Sinai. In: Said, Rushdi (Ed.), The Geology of Egypt. A.A. Balkema, Rotterdam, pp. 361—380.

Kashai, W., Shilo, A., Wolf, O., 1987. Northeastern Sinai — geology and oil exploration. In: Gvirtzman, G., Shmueli, A., Gross, Y., Ben Arieh, Y., Harel, M. (Eds.), Sinai Part 1 — Physical Geography. Ministry of Defense and Ha'Aretz Publ. House, pp. 149—164.

Kroitoru, L., 1980. The hydrogeology of the Nubian Sandstone in southern Israel. M.Sc. Thesis, Tel Aviv University, 45pp. (in Hebrew, English abstract).

Kronfeld, J., Rosenthal, E., Weinberger, G., Flexer, A., Berkowitz, B., 1993. The interaction of two major old water bodies and its implication on the exploitation of groundwater in the multiple aquifer system of central and northern Negev, Israel. J. Hydrol. 143, 169—190.

Lapidoth, Israel Oil Prospectors Corp. Ltd., 1976. Composite and stratigraphic logs for borehole Halal 1.

Livshitz, Y., 1999. The influence of natural and artificial factors on chemical composition of groundwater in the northwestern Negev and the southern portion of the Shfela. Unpublished Ph.D. Thesis, Ben-Gurion University of the Negev, 165pp.

Mills, A.C., Shata, A., 1989. Groundwater assessment of Sinai. Egypt Groundwater 27 (6), 793—801.

Movshovitz, M., Ben Zvi, A., 1973. Survey of water resources in the Qadesh Barnea area. Tahal, Tel Aviv, Rep 01/73/24, 23pp (in Hebrew).

Mualem, Y., 1971. Hydrological regional study of El Arish aquifer. Report of the Hydrological Service of Israel, Hydro/2/1971, Jerusalem, 85pp (in Hebrew).

Nada, A.A., Awad, M.A., 1991. Environmental isotopes, chemical composition and groundwater sources in El Maghara area, Sinai, Egypt. Isotopenpraxis 27 (4), 169—172.

Parkhurst, D.L., 1999. PHREEQC FAQ. Internet site of the USGS. http://wwwbrr.cr.usgs.gov/projects/GWC_coupled/phreeqc/faq.html.

Parkhurst, D.L., Appelo, C.A.J., 1999. User's Guide to PHREEQC (Version 2) — A Computer Program for Speciation, Batch-reaction, One-Dimensional Transport and Inverse Geochemical Calculations. USGS Water-Resources Investigation Report 99-4259, Denver, Colorado.

Rosenthal, E., 1987. Chemical composition of rainfall and groundwater in recharge areas of the Bet Shean—Harod multiple aquifer system. J. Hydrol. 89, 329—352.

Rosenthal, E., Weinberger, G., Berkowitz, B., Flexer, A., Kronfeld, J., 1992. The Nubian Sandstone aquifer in the western Negev, Isreal: delineation of the hydrogeological model under conditions of scarce data. J. Hydrol. 132, 107—135.

Rosenthal, E., Jones, B.F., Weinberger, G., 1998. The chemical evolution of Kurnub Group paleowater in the Sinai—Negev province — a mass balance approach. Appl. Geochem. 27 (3), 1—17.

Rosenthal, E., Weinberger, G., Kronfeld, J., 1999. Water salinization caused by residual Neogene and Pliocene Sea water: an example from the Judea Group aquifer, southern Israel. Ground Water 37, 261—270.

Rosenthal, E., Flexer, A., Möller, P., 2006. The paleoenvironment and the evolution of brines in the Jordan-Dead Sea transform and in adjoining areas. Int. J. Earth Sci. (Geol. Rundsch). 95, 725—740.

Said, R., 1962. The Geology of Egypt. Elsevier Publ. Co, Amsterdam.

Said, R., 1990. The Geology of Egypt. A.A. Balkema, Rotterdam/Brookfield.

Schoeller, H., 1956. Geochemie des equx souterraines. Application aux eaux des gisements de petrole. Soc. des Editions Technip, Paris, 156pp.

Shata, A., 1956. Structural development of the Sinai Peninsula. Egypt Desert Inst. Bull. 6 (2), 117—157.

Starinsky, A., Bielski, M., Ecker, A., Steinitz, G., 1983. Tracing the origin of salts in groundwater by Sr isotopic composition (the crystalline complex of the southern Sinai (Egypt). Isotope Geosci. 1, 257—267.

Water Resources Research Inst. and Japan International Cooperation Agency, 1992. Reports to the Egyptian Water Authority on Water Resources in Sinai, 53pp.

Weinberger, G., 1986. Sedimentary environments of the Lower Cretaceous in the northern Negev. Ph. D. Thesis, Tel Aviv University, 240pp (in Hebrew, English abstract).

Weinberger, G., 2003. Structural and lithofacial variables in the subsurface of the northern Negev and their bearing on the hydrogeology of the Kurnub and Judea Groups. Israel Water Commission, Rep.70/01 (in Hebrew), 20pp.

Weinberger, G., Rosenthal, E., Flexer, A., 1992. The subsurface geology of central and northern Negev with possible implications on the regional groundwater flow pattern. J. African Earth Sci. 14, 155—172.

White, D.E., 1960. Summary of chemical characteristics of some waters of deep origin. U.S. Geol. Surv. Prof. Pap. 400B, pp. 454.

Zaghloul, E.A., 1999. The hydrogeology of Upper Cretaceous Limestone aquifer at Areif el-Naqa area, East Central Sinai, Egypt. Ann. Geol. Surv. Egypt XXII, 501—509.

Zilberbrand, M., Rosenthal, E., Guttman, J., Weinberger, G., Fridman, V., 2005. Stages in updating a conceptual model of the Yarkon—Taninim basin: basin boundaries, hydrogeochemistry and salinization processes. Report of the Hydrological Service of Israel, pp. 49 (in Hebrew).